The origin, evolution and molecular diversity of the chemokine system

Alessandra Aleotti[1,2,*,#], Matthew Goulty[1,2,*,#], Clifton Lewis[1,2], Flaviano Giorgini[1,2] and Roberto Feuda[1,2,#]

[*]Equal contribution

[#]Author for correspondence: rf190@leicester.ac.uk; aa1176@leicester.ac.uk; mg478@leicester.ac.uk

[1]Neurogenetics Group

[2]Department of Genetics and Genome Biology University of Leicester, Leicester, United Kingdom

Keywords: Chemokine, Phylogeny, Evolution, Vertebrate, GPCR, Receptor, Ligand, CK, CKL, CKR, CKLF, TAFA, CYTL

ABSTRACT

Chemokine signalling performs key functions in cell migration via chemoattraction, such as attracting leukocytes to the site of infection during host defence. The system consists of a ligand, the chemokine, usually secreted outside the cell, and a chemokine receptor on the surface of a target cell that recognises the ligand. Several non-canonical components interact with the system. These include a variety of molecules that usually share some degree of sequence similarity with canonical components and, in some cases, are known to bind to canonical components and/or to modulate cell migration (1, 2). While canonical components have been described in vertebrate lineages, the distribution of the non-canonical components is less clear. Uncertainty over the relationships between canonical and non-canonical components hampers our understanding of the evolution of the system. We used phylogenetic methods, including gene-tree to species-tree reconciliation, to untangle the relationships between canonical and non-canonical components, identify gene duplication events and clarify the origin of the system. We found that unrelated ligand groups independently evolved chemokine-like functions. We found non-canonical ligands outside vertebrates, such as TAFA "chemokines" found in urochordates. In contrast, all receptor groups are vertebrate-specific and all - except ACKR1 - originated from a common ancestor in early vertebrates. Both ligand and receptor copy numbers expanded through gene duplication events at the base of jawed vertebrates, with subsequent waves of innovation occurring in bony fish and mammals.

INTRODUCTION

The chemokine system is responsible for regulating many biological processes, including host defence, neuronal communication and homeostasis (3–5). The system has two components, a ligand, usually a small cytokine called a chemokine, and a receptor. It typically operates through chemoattraction, wherein one cell type produces and secretes chemokines, creating a chemical gradient as these molecules disperse. Cells equipped with the corresponding chemokine receptors on their membranes can recognise and bind to specific chemokines, promoting their migration along the gradient (4). This mechanism allows cells to reach target locations, such as infection sites during inflammation or tissues important for homeostatic functions, e.g., leukocyte maturation and trafficking (3, 6). Chemokines involved in the latter homeostatic functions are usually constitutively expressed, while those involved in inflammatory responses have an inducible expression (7). Chemokine ligands are categorised into four groups, XC, CC, CXC, and CX3C, according to the pattern of cysteine residues in the N-terminal portion of the protein (8). Likewise, the receptors are classified based on the ligands they bind to into four groups, the XCR, CCR, CXCR, and CX3CR, and all of them belong to the GPCR class A superfamily (9). In addition to canonical components, other molecules have been discovered to function similarly to chemokine ligands (1) or receptors (2) (see Table 1). These include: the chemokine-like factor (CKLF) that binds to chemokine receptor CCR4 (10, 11) and drives cell migration *in vivo* (12); TAFA chemokines, expressed mainly in the nervous system, which share structural similarities to canonical chemokines (13, 14) and bind GPCRs related to chemokine receptors, e.g. formyl peptide receptors (15, 16) and GPR1 (17); Cytokine-like 1 (CYTL1) that binds CCR2 (18) and has been suggested to be related to CC ligands based on the presence of a IL8-like chemokine fold (19). There are also non-canonical chemokine receptors, such as: the chemokine-like receptor (CML1, or also CMKLR1) ((20); atypical chemokine receptors (ACKRs) (21); and viral chemokine receptors (22–25). Unlike other chemokine receptors, atypical receptors cannot initiate classical chemokine signaling upon ligand binding (21, 26). The human genome encodes four types of atypical chemokine receptors: the ACKR1 (also known as DARC), ACKR2 (also known as D6), ACKR3

(also known as CXCR7) and ACKR4 (also known as CCRL1) (27, 28). Additionally, several proteins of viral origins, such as US28 from human cytomegalovirus, have chemokine-receptor/binding activity (22, 23). These viral proteins can bind a wide array of chemokine ligands (23).

Despite the extensive research on the chemokine system, with over 320,000 papers available on PubMed, many aspects of its evolution remain unclear. For instance, the homology between canonical and non-canonical ligands is uncertain and supported by circumstantial evidence, such as shared specific motifs (12, 13, 19, 29). Furthermore, the relationships between canonical, atypical, and viral receptors and the outgroup of the canonical chemokine receptors remain uncertain. Finally, the evolutionary history of the canonical and non-canonical components remains poorly understood outside a few key model systems (9, 30, 31). These outstanding questions share common underlying causes, including the use of inadequate inference methods (such as relying solely on sequence similarities) and limited sampling of species (e.g., focusing mainly on humans, mice, and zebrafish (7, 32)). Additionally, solving the phylogenetic relationships for short molecules such as chemokine receptors and ligands is particularly challenging due to the lack of strong phylogenetic signals (33).

Here, to clarify these outstanding questions, we use state-of-the-art phylogenetic methods, including those designed for single-gene phylogenies, a large taxonomical sampling comprising both vertebrate and invertebrate genomes and the entire complement of canonical and non-canonical components of both receptors and ligands. Our findings substantially clarify the phylogenetic relationship between canonical and non-canonical ligands and receptors and suggest that unrelated proteins evolved “chemokine-like” ligand function multiple times independently. Additionally, we discovered that all the canonical and non-canonical chemokine receptors (except ACKR1) originated from a single duplication in the vertebrate stem group, which also gave rise to many GPCRs. Lastly, we characterized the complement of canonical and non-canonical components in the common ancestor of vertebrates and identified several other ligands and receptors with potential chemokine-related properties that could be explored in future functional work.

RESULTS

There are five unrelated groups of ligands.

Initially, we focused on the ligands, including all the canonical chemokines, the CYTL, the TAFAs and the CKLF Super Family (CKLFSF) proteins (Table 1). The presence of a four transmembrane MARVEL domain in the latter proteins (12, 34, 35) distinguishes them from canonical chemokines, the CYTL and the TAFAs. Therefore, we separated these two groups for further analysis. Using BLASTP or PSI-BLAST (36–38) (see Materials and Methods for more details) against 64 species from 19 animal phyla (Table S1), we identified 891 putative homologs for chemokines, TAFA and CYTL and 602 putative homologs of the CKLF Super Family.

We utilised CLANS (39, 40), a clustering tool based on sequence similarity and local alignment, to identify homology within these two groups. Unlike traditional phylogenetic methods, CLANS assigns homology between sequences based on BLAST and customisable stringency levels defined according to p-values (39). When two (or more) sequences are connected at a lower p-value (closer to 0), this indicates a high level of homology. Conversely, if two or more sequences only connect at a higher p-value, this suggests a relatively low level of sequence homology. Our analysis shows that canonical chemokines form a distinct group with a clear distinction between C-X-C-type and C-C-type (Figure 1A). Whereas CXCL17, TAFA and CYTL remain separate from canonical chemokines and from each other even at the loosest p-values tested (Figure 1A). The distinction between CXCL17 and all other canonical chemokines is consistent with our receptor results, showing that the potential receptor for CXCL17, GPR35 (41), is also not within the canonical chemokine receptor group (see below). However, it is important to note that recent studies fail to demonstrate CXCL17 activity at GPR35 (42, 43). Within the CKLFSF, two large clusters were identified, named CKLF I and CKLF II, although these ultimately connect to form one large superfamily (Figure 1B). These clusters are robust to the different stringency thresholds used (Figures S1 and S2 and Materials and Methods for further details). Our results indicate that even when the stringency level to detect

homology is relaxed, canonical chemokines, TAFA, CYTL, and CXCL17 remain in distinct clusters. This suggests that, similarly to CKLFs, these proteins are not homologous and convergently evolved chemokine-like properties. We have thus identified five distinct groups of ligands: i) the canonical chemokines, ii) TAFA "chemokines", iii) CYTL, iv) CXCL17, and v) CKLF Super Family (Figure 1A and 1B).

The evolution of chemokine and chemokine-like ligands in animals.

To better understand the evolution of both canonical and non-canonical chemokine ligands, we performed a separate phylogenetic reconstruction for each group (Figure 1C, D and Figures S8-17) (see methods for details). To evaluate the nodal support, in addition to the UltraFast bootstrap (UFB) (44, 45), we used Transfer Bootstrap Expectation (TBE), a method that has been developed for single-gene phylogeny (46). To evaluate ortholog/paralog relationships and overall dynamics of the ligand complement, we used GeneRax (47). This new method uses maximum likelihood to reconcile the gene tree with the species tree (47). In brief, given a gene and species tree, GeneRax uses a maximum likelihood approach to optimise the duplication and loss events (47, 48).

Our analysis initially identified a few invertebrate putative chemokine ligands (Figure 1A), however, these sequences lacked protein signatures associated with the canonical ligands (Figures S3-5 and File S3), and they were therefore excluded from further analysis (see Supplementary Results for further information). The phylogenetic tree for the canonical ligands identifies two major groups, the CC-type, which also includes the XC- and X3C-types, and the CXC-type (TBE = 0.95, UFB = 92%) (Figure 1C and Figures S8,9), confirming the previous finding obtained using synteny data (49, 50). Next, to clarify the distribution of canonical chemokines, we first reconciled their gene tree with the species tree and then used the reconciled tree to trace the presence/absence of each chemokine group throughout all the species (Figure 2A and Figure S18). Our results confirm previous findings that canonical chemokines are uniquely present in vertebrates (30, 49). Additionally, they indicate that chemokines are not evenly distributed across vertebrates and can be different even between closely related species (51). Some are very ancient, e.g., CXCL12 is present in lamprey; CXCL14 and

141 CCL20 are present in all jawed vertebrates; and CXCL8 is present throughout bony fishes and
142 tetrapods, with few exceptions, notably mice and rats. However, a large part of the chemokine
143 diversity evolved within mammals (e.g., CXCL1/2/3, CXCL16, and CCL25), particularly placentals (e.g.,
144 CXCL5/6 and CCL3/18). The phylogenetic relationships we uncovered in our reconciled tree were
145 mostly compatible with known syntenic relationships as described in human (7). For example, the
146 large cluster of CXC-type chemokine genes present in human chromosome 4 contains CXCL1-11 plus
147 CXCL13 (7), all of which coalesce within a monophyletic group in our tree (Figure 2A). The micro-
148 synteny within this cluster is also, to some extent, reflected in the phylogenetic relationships.
149 Similarly, the other large syntenic cluster of chemokines, located on human chromosome 17,
150 containing most of the CC-type chemokines (7), corresponds, with few exceptions, to a large
151 monophyletic clade in our tree (Figure 2A). CXCL16 which is on a nearby locus of chromosome 17, is
152 also phylogenetically related to this CC-type clade (Figure 2A). The complement of the canonical
153 chemokines undergoes the largest expansion at the base of jawed vertebrates, where there is an
154 expansion from 4 to 18 genes (Figure 2B). A second expansion occurred at the base of bony fishes
155 (i.e., Osteichthyes) followed by relative stability until placental mammals, where the total number of
156 canonical chemokine ligands jumped to 45 genes. Finally, unlike previous works (52) our results
157 support the presence of orthologs of both CC-type and CXC-type in the common ancestor of all
158 vertebrates (Figure 2A).

159 Differently from the canonical chemokines, we identified a *bona fide* TAFA, i.e., with specific
160 protein motifs, in the urochordates, the sister group to vertebrates (see Supplementary Results and
161 Figures S6-7). The phylogenetic trees (Supplementary Figures S10,11) identified monophyletic
162 groups for TAFA5 (TBE=0.98, UFB=98%), TAFA1 (TBE=0.94, UFB=98%), TAFA4 (TBE=0.77, UFB=75%)
163 and TAFA2/3 (TBE=0.65, UFB=84%). The reconciled tree from GeneRax places the root at the
164 urochordate sequence (Figure S19), therefore clarifying that the TAFA5 clade is the sister group to
165 TAFA1-4 (Figure 2A). The family originated in the ancestor of urochordates and vertebrates, and the
166 first duplications occurred at the base of vertebrates giving rise to the TAFA5 split followed by the

167 TAFA1 split. Subsequently, at the base of jawed vertebrates, additional duplications bring the
168 complements from 3 to 10 (Figure 2B), giving rise to the remaining groups so that all jawed
169 vertebrates possess the full diversity of TAFAs.

170 The phylogenetic trees for CYTL and CXCL17 mainly reflect the species trees (Figures S12-15),
171 and the reconciliations revealed very simple complement dynamics (Figure 2B and Figures S20,21).
172 However, these molecules show a remarkable difference in their distribution. CYTLs are present
173 throughout gnathostomes, while CXCL17 is found only in placental mammals (Figure 2A).

174 The phylogenetic analysis for the CKLF super family (Figure 1D and Figures S16,17) recovered
175 a monophyletic clade for the CKLF I group (TBE=0.96, UFB=80%) that we had already identified
176 through CLANS. This group contains CKLF, which is known to interact with C-C chemokine receptor 4
177 (10, 11), as well as CMTM1, 2, 3, 5, and proteolipid protein 2 (PLP2). Other monophyletic clades that
178 are consistent with the CLANS are CMTM4/6 (TBE=0.90, UFB=61%), CMTM7 (TBE=0.92, UFB=83%)
179 and a clade containing CMTM8 plus other related molecules such as plasmolipin (PLLP) and myelin
180 and lymphocyte proteins (MAL) (TBE=0.89, UFB=60%). The latter were all part of a large cluster that
181 we called CKLF II in the CLANS (Figure 1B). However, the placement of the root of the tree in Figure
182 1D can affect the interpretation of the relationships among CKLF II subgroups. To address this
183 problem and clarify the patterns of duplications and the presence/absence of each group
184 throughout animals, we used GeneRax to reconcile the gene with the species tree (see above and
185 Material and Methods for details). Our results suggest (Figure 2 and Figure S22) that most CKLFSF
186 groups, such as CMTM4,6 and 8, originate in the vertebrate stem group from pre-existing CMTM
187 genes and are widely distributed in animals. The CKLF I subgroups originate from duplications at the
188 base of jawed vertebrates, except for the split between CKLF and CMTM1 that occurs only within
189 mammals (Figure 2A). We observe the major two expansions of the CKLFSF genes in the stem group
190 of vertebrates (from 6 to 10 complements), and then in jawed vertebrates (from 10 to 16
191 complements). Interestingly, the extent of these expansions are less drastic than those we see for

192 canonical chemokines (Figure 2B). In total, we have identified that the five distinct ligand groups
193 have a different origin in the animal tree of life and underwent divergent evolutionary histories.

194 **Canonical and non-canonical chemokine receptors are divided into four groups.**

195 Next, we investigated the origin and pattern of duplication for the chemokine receptors and
196 chemokine-like receptors (Table 1). Using BLASTP against the 64 species, we identified 7,157
197 putative chemokine receptors (see Materials and Methods for more details) and investigated their
198 relationships using CLANS (see above for justification). The result (Figure S23C) identifies four main
199 groups of chemokine receptors and chemokine-like receptors. The first comprises canonical
200 receptors (i.e., CCR, CXCR, CX3CR1, CX3C, and XCR1), and the second includes atypical receptor 3
201 and GPR182, which has been recently shown to have chemokine receptor activity (53). The third
202 group, which we named Chemokine-like plus (CML-plus), contains the chemokine-like receptors
203 (CML1 also known as chemerin receptor 1), formyl peptide receptors (FPR) that bind the TAFA
204 ligands (15, 16) and other GPCRs such as GPR1 (chemerin receptor 2), GPR33, PTGDR2. Furthermore,
205 the CLANS analysis identifies an intermediate group containing angiotensin, apelin and other
206 receptors and shows sequence similarity to canonical and chemokine-like receptors (Figure S23B).
207 Finally, our analysis identifies a small cluster composed of only ACKR1 that do not connect to other
208 GPCRs or other atypical receptors even at loose p-value thresholds. This indicates that their
209 sequence is either non-homologous or highly divergent from other chemokine receptors and
210 atypical receptors. Overall, these groups are robust to the stringency threshold used (i.e., different
211 p-values) (Figure S23). Interestingly, no specific cluster of viral or viral-like receptors was identified,
212 but 6 of the reference viral receptor sequences clustered with the canonical chemokine receptors.

213 Altogether, these results confirm the homology between the canonical receptors and
214 atypical receptor 3/GPR182. However, these findings indicate that the other GPCRs, such as the
215 chemokine-like receptors, formyl peptide receptors, GPR1, and GPR33, are also closely related to the
216 canonical receptors. Remarkably, these results also indicate that ACKR1 is not homologous to the

217 canonical chemokine receptors. Furthermore, all clusters of chemokine receptors contained only
218 vertebrate sequences, except for the receptors of viral origin.

219 **Canonical and chemokine-like receptors derive from single gene duplication in the ancestor of**
220 **vertebrates**.

221 Previous studies suggested that the chemokine receptors evolved from a duplication of
222 angiotensin receptors (54) or adrenomedullin receptors (30, 55). However, these works were based
223 on error-prone phylogenetic methods such as Neighbour Joining (55). Our CLANS results indicate
224 that chemokine receptors and chemokine-like receptors have only been observed in vertebrates.
225 Therefore, we need to focus on invertebrate genomes to clarify the chemokine receptor's outgroup.
226 To clarify this, we lowered the p-value thresholds of CLANS (to p-value < $1e^{-50}$) and collected a
227 combined dataset including all chemokine receptor sequences and outgroups (i.e., sequences that
228 connect to the chemokine receptor cluster), resulting in 3,026 sequences. We then performed a
229 phylogenetic tree on this dataset using maximum likelihood methods with UFB and TBE for
230 evaluating nodal support (see above and Materials and Methods for details).

231 Our combined phylogenetic analysis shows strong support for the monophyly of canonical
232 chemokine receptors (UFB=96, TBE=1.0), the CML-plus (UFB=95, TBE=0.99) and the atypical
233 3/GPR182 (UFB=100, TBE=1) (Figure 3, S24 and S25). In contrast, viral chemokine receptors are
234 paraphyletic, with three sequences placed within the canonical chemokine receptors and 3 forming
235 a monophyletic group sister to them (UBF=84 TBE=1.0). Our results also suggest that the
236 intermediate group, which includes apelin receptors, angiotensin receptors, bradykinin receptors,
237 and orphan GPCRs (e.g., GPR25; GPR15) forms a monophyletic clade with the canonical chemokine
238 receptors, CML-plus group and atypical3/GPR182 (UFB=61, TBE=0.91). However, its position changes
239 between the sister group to canonical chemokine receptors plus atypical3/GPR182 in the TBE tree
240 (TBE=0.84) and sister to CML plus in the ultrafast bootstrap tree (UFB=38).

241 All the groups mentioned above form a large clade composed of vertebrate-specific GPCRs
242 (UBF=100 TBE=0.96) that also includes other GPCRs, such as CLTR and P2RY receptors (Figure 3, S24

243 and S25). Another orphan GPCR, GPR35, had been proposed as a potential chemokine receptor (41);
244 however, this was later questioned (42, 43) and GPR35 is still generally considered orphan (56–58).
245 Our analysis collected GPR35 and placed it within this large vertebrate specific clade indicating that
246 is it also a vertebrate specific gene but not phylogenetically a 'canonical' chemokine receptor. The
247 closest outgroup to this clade is composed of a few sequences from urochordates, the sister group
248 of vertebrates (UFB=49 TBE=0.91) (Figure 3, S24 and S25). Interestingly, as the sister group of this
249 clade, we identify a group composed of Relaxin receptors, which contain sequences from both
250 urochordates and vertebrates (UBF=53 TBE=0.95). Finally, as the sister group of these large clades,
251 we identified a clade of cephalochordate-specific sequences (UBF=44).

252 To clarify the duplication pattern and origin of the chemokine receptors, we used GeneRax
253 (47) (see Materials and Methods). Our results indicate (Figure 4A, S26) that all chemokine receptors
254 (except ACKR1) originated from a duplication in the stem lineage of vertebrates. This duplication of
255 an unknown GPCR gave rise to the CML-plus, the canonical chemokine receptors and atypical
256 3/GPR182 groups as well as the intermediate group and other GPCRs (Figure 4A, S26). This result is
257 consistent with the distribution of the paralogous Relaxin receptors which are present both in
258 urochordates and vertebrates and the position of the orphan urochordate sequences as sister group
259 of canonical chemokine receptors, CML-plus group and atypical3/GPR182 and other GPCRs (see
260 above). Furthermore, the phylogenetic relationships amongst canonical chemokine receptors are
261 overall consistent with the syntenic gene patterns known in human (7). The largest cluster of
262 chemokine receptor genes spans 3 closely located loci on human chromosome 3 (7). It includes most
263 CCRs, XCR, and CX3CR and corresponds to one of the two major monophyletic clades in our tree
264 (Figure 4A). Another example is the mini cluster of CXCR1 and CXCR2, located on human
265 chromosome 2 (7), which we also found to form a monophyletic clade (Figure 4A).

266 We used the reconciliation to better understand the repertoires of receptors present at key
267 nodes during vertebrate evolution. Our results (Figure 4B) show a substantial difference in the
268 duplication pattern of different receptor families. For example, the complement of the

atypical3/GPR182 remains constant throughout vertebrate evolution while the canonical and chemokine-like receptor groups expanded dramatically. The canonical chemokine receptors expanded from 5 to 20 genes and the CML-plus from 1 to 11 in the ancestor of the jawed vertebrates (Figure 4B). The expansion of the canonical CKRs is also not evenly distributed across its subgroups, with the ancestral CC type receptors undergoing a series of duplications in jawed vertebrates while the CXCR paralogs did not, specifically one (CXCR4) remains in single copy across all vertebrates. We inferred that in the stem lineage of vertebrates, five canonical chemokine receptor paralogs had already diverged, representing the two major types of receptors (2 CCR and 3 CXCR paralogs). Also, present in the stem lineage of vertebrates were ACKR3 and GPR182 as well as a single copy gene which would later diverge to produce all the CML-plus clade.

DISCUSSION

This work substantially clarifies the evolutionary assembly of the chemokine system. Our analysis shows that contrary to the receptors which evolved from a single duplication event in the vertebrate stem group, several unrelated molecules acquired the ability to interact with chemokine receptors over the course of evolutionary history. Furthermore, our results (summarized in Figure 5) suggest that the key components of the chemokine system, including the chemokine receptors themselves, evolved in the stem group of vertebrates in the Cambrian around 500 million years ago and then underwent substantial diversification in the stem group of jawed vertebrates. These findings shed new light on the complex evolutionary history of the chemokine system.

Unrelated molecules converged to chemokine function.

Based on the presence of shared protein motifs, TAFA “chemokines” (13, 14), CXCL17 (59, 60) and CYTL (19) have been proposed to be homologous to chemokine ligands. However, our findings strongly suggest that these molecules are not homologous (Figure 1) and likely acquired the ability to activate a chemokine-like response through convergent evolution. Our conclusions differ from those previous studies (13, 19, 59, 60) due to the differences in data completeness and

methodological approach. Specifically, we used a complete set of canonical and non-canonical ligands and assessed the homology using overall sequence similarity rather than single motifs. Our results support and expand upon the findings of (29), which suggested that the presence of a CXC or CC motif is necessary but not sufficient for a protein to be defined as a chemokine ligand. Similarly, CKLF has been considered a "new member" of the chemokine family based on its function (12) we argue that classification based solely on function is insufficient and can be misleading. Instead, we recommend considering the evolutionary relationships among these molecules as the primary criterion for classification.

Most of the canonical and non-canonical ligands are vertebrate innovations.

Our results clarify the distribution of canonical chemokine ligands in animals (Figure 2) and confirm that they are present only in vertebrates (30). We identify orthologs of CXCL and CCL ligands in both extant lineages of cyclostomes (Figure 2A). While chemokines have already been described in lamprey (52, 61, 62), it is the first time, to our knowledge, that they are described also in hagfish. Our findings also indicate that both CC and CXC types were present in the common ancestor of all vertebrates and that few ancestral genes gave rise to the entire diversity of ligands that we know in current animals. Furthermore, our results indicate that many chemokines, such as CXCL1-7, CXCL16, as well as CCL25, CCL11/13, and CCL2/7, are uniquely present in mammals, suggesting that the mammal ligand repertoire is substantially more complex than the one observed in other vertebrates.

Regarding non-canonical chemokine-like families, our findings indicate that the TAFA family originated in the ancestor of vertebrates and urochordates; CYTL is a novelty of jawed vertebrates; and CXCL17 is mammal-specific and likely unrelated to canonical chemokines (similar to its controversial putative receptor, GPR35 (41–43), that is not a canonical chemokine receptor). The CKLF superfamily has a more complex pattern with the presence of few groups in invertebrates and then great expansions occurring at the base of vertebrates. The CKLFSF includes a monophyletic clade (CKLF group I) comprising the original CKLF that binds CCR4, as well as CMTM1,2,3,5, derived from duplications at the jawed vertebrates stem group. Interestingly, our analysis also revealed that

321 additional molecules not previously considered part of the CKLF super family are closely related to
322 classic members and should be included in it. For example, proteolipid protein 2 (PLP2) belongs to
323 the CKLF I group and is, therefore more closely related to the CKLF with chemokine function than
324 several other CKLFSF members. Similarly, CMTM8 is more closely related to plasmolipin (PLLP) and
325 myelin and lymphocyte protein (MAL) than to any of the classic CKLFSF members. Although this
326 relationship had been proposed based only on sequence similarity (34), our phylogenetic analysis
327 provides additional evidence for it. Therefore, the potential chemokine function of all these
328 additional members should be explored *in vitro* and *in vivo* in both vertebrates and invertebrates.

329 **Most receptors derive from a single gene duplication.**

330 Our results clarify the distribution of canonical chemokine receptors in vertebrates (Figure
331 4), and their evolutionary relationships and identify the pattern of duplication that leads to their
332 origin (Figure 4A, S26). Unlike previous works (63), we identify that atypical receptors do not form a
333 monophyletic group. Specifically, atypical 2 and 4 are part of the canonical clade specifically related
334 to CC-type receptor subclades. Furthermore, we find that the atypical 3 receptors are related to
335 GPR182, supporting previous functional data suggesting that the latter are atypical chemokine
336 receptors binding CXCL10, 12, and 13 (53). We attribute these differences to our use of wider GPCR
337 sampling and improved methods for phylogenetic inference.

338 Remarkably, our results do not identify ACKR1 as related to the main chemokine receptors
339 but rather as a divergent clade (Figure S23). To our knowledge, this is the first time this observation
340 has been made. Our current results do not allow us to clarify the evolutionary origin of ACKR1.
341 However, the presence of 7TMD domains suggests that they are GPCRs that independently acquired
342 the ability to bind chemokines. Alternatively, similarly to other genes evolved in the immune system,
343 ACKR1 may have been subjected to strong selective pressures that substantially changed their
344 sequence, obscuring their phylogenetic relationships. The case of ACKR1 being the most distantly
345 related receptor is intriguing as it is one of the most promiscuous chemokine receptors (2, 64) and it
346 has been shown to bind both CC and CXC chemokines (65, 66).

Viral chemokine receptors represent a cryptic group that can bind multiple chemokines (22, 23). Despite their functional similarity to canonical chemokine receptors, viral chemokine receptors' evolutionary origin and distribution remain poorly understood. Our results indicate that viral GPCRs do not form a monophyletic group, suggesting that the ability to encode chemokine-like receptors has evolved independently in multiple viruses, including cytomegaloviruses and poxviruses. The placement of viral sourced sequences within an otherwise vertebrate-specific clade supports the hypothesis that viruses acquired these genes through non-vertical inheritance. Given the paraphyly of viral receptors, this appears to have occurred multiple times. However, there are significant uncertainties and further work is needed to untangle details of viral chemokine receptors' evolution.

Our analysis reveals that the clade comprising apelin receptors, angiotensin receptors, bradykinin receptors, and orphan GPCRs (shown in Figure 3, 4 and S24–26) is closely related to chemokine receptors. This finding partially supports previous studies (54) that suggested a gene duplication event gave rise to both chemokine receptors and angiotensin receptors. Interestingly, we found that single gene duplication in the vertebrate stem group led to the emergence of canonical receptors and atypical 2,3,4, GPR182, chemokine-like receptors, formyl peptide receptors, the intermediate group, and many other known and orphan GPCRs including the controversial putative CXCL17 receptor GPR35. These findings suggest that two rounds of genome duplication (67, 68) played a role in the expansion of GPCR gene families. Future research will focus on investigating the functions of the orphan genes and many-to-one orthologs discovered in urochordates. This will provide further insight into the evolution and diversification of GPCR families in vertebrates.

The molecular assembly of the chemokine system

In this work, we explored the evolution of both ligand and receptor components of the chemokine signaling system, including non-canonical molecules with either chemokine-like function or sequence similarity. Our analysis suggests that the canonical chemokine signaling evolved in the vertebrate stem group (about 500 Mya) likely due to the two rounds of genome duplication that gave rise to many vertebrate novelties (67, 68). We found that the ancestral vertebrate repertoire

373 included orthologs of both major ligand groups (CXCL and CCL) and both CCR and CXCR receptors
374 and non-canonical components such as TAFA and CKLFSF ligands, and the receptors Atypical 3 and
375 GPR182 (Figure 5). The distribution of ligands and receptors in the ancestor of all vertebrates seems
376 to confirm the hypothesis that the ancestral function of chemokines was homeostatic (e.g., CXCL12,
377 CXCL14) with inflammatory functions arising from recent duplications (e.g., CXCL5, CXCL6),
378 potentially reflecting a rapid evolution induced by the selective pressure of new pathogens (7).
379 Chemokine ligand and receptor genes are known to cluster on specific chromosomes (7), consistent
380 with the hypothesis that they may be the result of the combination of *en bloc* duplication followed
381 by tandem duplications (30, 49, 50). Due to limited high-quality genomes, syntenic patterns of
382 chemokine genes described so far are based primarily on humans and a handful of other species (30,
383 49, 50), hampering our understanding of the level of conservation of these syntenic patterns.
384 Conversely, our large-scale phylogenetic analyses encompassed many species. We uncovered
385 several phylogenetic relationships that are consistent with known syntenic patterns in human,
386 providing stronger evidence for their evolutionary relationship.

387 The evolutionary history of canonical components includes several examples of known
388 ligand-receptor pairs following a corresponding pattern of origin and temporal dynamics of
389 duplications. This is true for example, for the ancient homeostatic CXCL12 ligand and its
390 corresponding receptors CXCR4 and ACKR3, that all originated in early vertebrates (7). The early
391 origin and conservation of CXCR4 and CXCL12 in the ancestor of vertebrates is interesting as this pair
392 plays a key role in the migration of neural crest cells (69) - a key vertebrate innovation (70). This
393 combined with the fact that homeostatic chemokine ligands/receptors tend to be restricted to
394 monogamous pairing (2, 51) suggests that homeostatic chemokine pairings are more ancient and
395 conserved being in single copy throughout much of the vertebrates. Contrastingly, inflammatory
396 chemokine pairings are more promiscuous, and this could be linked to the more recent duplications
397 in the genes, such as for CCL2/7/8/11/13 (Figure 2A) and their receptors CCR1/2/3/4/5 (Figure 4A).
398 For many of the non-canonical components, however, the ligand-receptor interactions are largely

unclear, and their pattern throughout vertebrate evolution remains to be explored. Overall, our results indicate that three waves of molecular innovation in the vertebrates, jawed vertebrates, bony fishes and mammal stem group increased the chemokine system's molecular complexity (Figure 5), allowing for the fine-tuning present in modern-day animals.

MATERIALS AND METHODS

Data Mining and Dataset Assembly. We collected 64 proteomes from 25 vertebrates, six chordates and 33 other animals covering the whole animal tree (Table S1). BUSCO v4.0.6 (71, 72) and the metazoa_odb10 set of 954 genes were used to evaluate their completeness (Table S1).

To identify potential homologs of canonical chemokines, TAFA chemokines and CYTL1, we used 207 curated sequences that we obtained from SwissProt (73, 74) as seeds for an initial BLASTP (36, 38) with e-value < e^{-10}. To identify putative chemokines in cyclostomes, the lamprey *Petromyzon marinus* (75) and the hagfish *Eptatretus burger* (76), we loosened the e-value to 0.05. Where putative chemokine sequences were found for one cyclostome species but not the other, those sequences were used to search again the other species. Furthermore, to investigate the presence of ligands outside vertebrates, we performed an additional BLASTP on invertebrate proteomes with an even looser e-value (0.1) and collected only up to five hits. This provided 18 initial candidate homologs spanning multiple invertebrate phyla. Further characterisation of these invertebrate sequences, through BLASTP versus SwissProt, protein domains search with InterProScan (77, 78), position in CLANS analysis (see below) and, where necessary, multiple sequence alignments, led us to retain only one urochordate sequence as a putative TAFA homolog (see Supplementary Results for details).

To identify homologs for the CKLF superfamily, we used 21 SwissProt-reviewed sequences. In addition to the BLASTP search, we used a position-specific iterative BLAST (PSI-BLAST) (37) with an e-value threshold of <e^{-10}. Using this approach, we identified a total of 590 putative homologs, including 186 from invertebrates.

We used BLASTP using 178 manually annotated receptor sequences from SwissProt as query sequences for the chemokine receptors. This includes all human canonical and atypical chemokine receptors (79). We also collected 8 viral sequences with chemokine receptor activity from UniProt (80) and performed a second BLASTP. We extracted all BLAST hits with e-values < e^{-10} and used Phobius (81) to predict their transmembrane domain structure. Only sequences with 5-8 transmembrane domains were kept. Hit sequences were annotated by their top 5 BLAST hits against SwissProt. All hits from both BLASTs were merged and filtered by cd-hit (82, 83) to remove redundant sequences at the 95% similarity threshold. This resulted in 7,157 putative chemokine GPCR sequences.

Identification of subgroups with Cluster Analysis of Sequences (CLANS). We utilised CLANS (39, 40) with default parameters and different p-values (i.e., stringency values) to visualize the relationships between subgroups of ligands and receptors. We assessed the similarity and interrelationships between different clusters by gradually relaxing the p-value threshold (Figures S1, S2 and S23). Additionally, we annotated each cluster using gene annotations for key species *Homo*, *Mus*, *Gorilla*, *Gallus, Anolis* and *Danio*. In the case of the receptors, to improve the cluster annotation all human Class-A GPCRs (excluding olfactory receptors) from GPCRdb (84) were added to the dataset as well as the 8 seed viral chemokine receptors from UniProt (80).

Alignment and phylogenetic analysis

Alignment. All ligand and receptor sequences were aligned using MAFFT (85, 86) with the --auto setting and using trimAl (87) to remove positions with >70% gaps.

Gene Trees. All gene alignments were analysed using IQTREE2 (88), the model test algorithm (89) was used to select the best substitution model for each analysis. Best models selected by IQTREE2 for each set are listed in Table S2 (for receptors we manually selected GTR20+F+G4 as the model as

it was a large dataset). Nodal support was estimated using 1,000 ultrafast bootstrap (44, 45) replicates. All analyses were repeated to run 100 non-parametric bootstrap repeats to calculate nodal support with transferable bootstrap expectation: which is specifically designed to account for phylogenetic instability (46).

For the receptors, due to the high computational burden of running TBE analyses on sequence-dense datasets, we first analysed the full set of 3,026 sequences connected in CLANS at a p-value of $< 1\ e^{-50}$ using UFB (Figure S25). Then, we extracted the chordate-specific clade sequences, including all chemokine receptor groups and their immediate outgroups, to analyse using TBE.

Gene tree species tree reconciliation. To understand the pattern of duplication and the evolution of gene complement we used GeneRax (47). GeneRax requires a gene tree that was obtained as described above and a species tree that we constructed manually using publicly available information. In the instances where the genes tree contained polytomies, we used ETE3 (90) to solve them. The undated DL mode and the closest approximation of the best-fitting substitution model were used for each alignment. To track the evolution of sub-lineages within each group, we used annotated sequences of key species (e.g., *Homo sapiens* and *Mus musculus*) as reference. For the receptors, we used only the chordate-specific clade subtree and sequences due to the computational burden of running GeneRax on a high number of sequences. For species tree-gene tree reconciliation, we treat the viral sequences as human sequences.

DATA AVAILABILITY

Supplementary material and raw output files for all the analyses described in this paper are available in the GitHub page: Roberto-Feuda-Lab/Chemokine2023 (github.com).

ACKNOWLEDGEMENTS

This work is supported by a University Research Fellowship (UF160226) to RF. AA is supported by a Research Grant from the Royal Society to RF (RGF\R1\181012). MG is supported by a PhD

Scholarship from the University of Leicester. CL is supported by a BBRSC MIBPT fellowship. This research used the ALICE High-Performance Computing Facility at the University of Leicester.

REFERENCES

1. K. Zhang, S. Shi, W. Han, Research progress in cytokines with chemokine-like function. *Cellular & Molecular Immunology* **15**, 660–662 (2018).
2. K. Chen, *et al.*, Chemokines in homeostasis and diseases. *Cell Mol Immunol* **15**, 324–334 (2018).
3. X. Blanchet, M. Langer, C. Weber, R. Koenen, P. von Hundelshausen, Touch of Chemokines. *Frontiers in Immunology* **3**, 175 (2012).
4. P. López-Cotarelo, C. Gómez-Moreira, O. Criado-García, L. Sánchez, J. L. Rodríguez-Fernández, Beyond Chemoattraction: Multifunctionality of Chemokine Receptors in Leukocytes. *Trends in Immunology* **38**, 927–941 (2017).
5. P. B. Tran, R. J. Miller, Chemokine receptors: signposts to brain development and disease. *Nature Reviews Neuroscience* **4**, 444–455 (2003).
6. B. Moser, M. Wolf, A. Walz, P. Loetscher, Chemokines: multiple levels of leukocyte migration control. *Trends in Immunology* **25**, 75–84 (2004).
7. A. Zlotnik, O. Yoshie, The Chemokine Superfamily Revisited. *Immunity* **36**, 705–716 (2012).
8. A. Zlotnik, O. Yoshie, Chemokines: A New Classification System and Their Role in Immunity. *Immunity* **12**, 121–127 (2000).
9. H. Nomiyama, N. Osada, O. Yoshie, A family tree of vertebrate chemokine receptors for a unified nomenclature. *Developmental & Comparative Immunology* **35**, 705–715 (2011).
10. Y. Wang, *et al.*, Chemokine-like factor 1 is a functional ligand for CC chemokine receptor 4 (CCR4). *Life Sciences* **78**, 614–621 (2006).
11. Y. Wang, *et al.*, Two C-terminal peptides of human CKLF1 interact with the chemokine receptor CCR4. *The International Journal of Biochemistry & Cell Biology* **40**, 909–919 (2008).
12. D.-D. Liu, *et al.*, Progress in pharmacological research of chemokine like factor 1 (CKLF1). *Cytokine* **102**, 41–50 (2018).
13. Y. Tom Tang, *et al.*, TAFA: a novel secreted family with conserved cysteine residues and restricted expression in the brain. *Genomics* **83**, 727–734 (2004).
14. D. C. Sarver, X. Lei, G. W. Wong, FAM19A (TAFA): An Emerging Family of Neurokines with Diverse Functions in the Central and Peripheral Nervous System. *ACS Chem. Neurosci.* **12**, 945–958 (2021).
15. W. Wang, *et al.*, FAM19A4 is a novel cytokine ligand of formyl peptide receptor 1 (FPR1) and is able to promote the migration and phagocytosis of macrophages. *Cell Mol Immunol* **12**, 615–624 (2015).
16. M. Y. Park, *et al.*, FAM19A5, a brain-specific chemokine, inhibits RANKL-induced osteoclast formation through formyl peptide receptor 2. *Sci Rep* **7**, 15575 (2017).

17. C. Zheng, *et al.*, FAM19A1 is a new ligand for GPR1 that modulates neural stem-cell proliferation and differentiation. *The FASEB Journal* **32**, 5874–5890 (2018).
18. X. Wang, *et al.*, Cytokine-like 1 Chemoattracts Monocytes/Macrophages via CCR2. *The Journal of Immunology* **196**, 4090–4099 (2016).
19. A. Tomczak, M. T. Pisabarro, Identification of CCR2-binding features in Cytl1 by a CCL2-like chemokine model. *Proteins: Structure, Function, and Bioinformatics* **79**, 1277–1292 (2011).
20. T. Yoshimura, J. J. Oppenheim, Chemokine-like receptor 1 (CMKLR1) and chemokine (C–C motif) receptor-like 2 (CCRL2); Two multifunctional receptors with unusual properties. *Experimental Cell Research* **317**, 674–684 (2011).
21. R. Bonecchi, G. J. Graham, Atypical Chemokine Receptors and Their Roles in the Resolution of the Inflammatory Response. *Frontiers in Immunology* **7**, 224 (2016).
22. T. N. Kledal, M. M. Rosenkilde, T. W. Schwartz, Selective recognition of the membrane-bound CX3C chemokine, fractalkine, by the human cytomegalovirus-encoded broad-spectrum receptor US28. *FEBS Letters* **441**, 209–214 (1998).
23. T. F. Miles, *et al.*, Viral GPCR US28 can signal in response to chemokine agonists of nearly unlimited structural degeneracy. *eLife* **7**, e35850 (2018).
24. M. M. Rosenkilde, M. J. Smit, M. Waldhoer, Structure, function and physiological consequences of virally encoded chemokine seven transmembrane receptors. *British Journal of Pharmacology* **153**, S154–S166 (2008).
25. H. Daiyasu, W. Nemoto, H. Toh, Evolutionary Analysis of Functional Divergence among Chemokine Receptors, Decoy Receptors, and Viral Receptors. *Frontiers in Microbiology* **3** (2012).
26. M. Meyrath, *et al.*, The atypical chemokine receptor ACKR3/CXCR7 is a broad-spectrum scavenger for opioid peptides. *Nature Communications* **11**, 3033 (2020).
27. R. J. B. Nibbs, G. J. Graham, Immune regulation by atypical chemokine receptors. *Nat Rev Immunol* **13**, 815–829 (2013).
28. F. Bachelerie, *et al.*, New nomenclature for atypical chemokine receptors. *Nat Immunol* **15**, 207–208 (2014).
29. S. S. Denisov, CXCL17: The Black Sheep in the Chemokine Flock. *Frontiers in Immunology* **12**, 2811 (2021).
30. M. E. DeVries, *et al.*, Defining the Origins and Evolution of the Chemokine/Chemokine Receptor System. *The Journal of Immunology* **176**, 401 (2006).
31. B. Bajoghli, Evolution and function of chemokine receptors in the immune system of lower vertebrates. *European Journal of Immunology* **43**, 1686–1692 (2013).
32. H. Nomiyama, *et al.*, Extensive expansion and diversification of the chemokine gene family in zebrafish: Identification of a novel chemokine subfamily CX. *BMC Genomics* **9**, 222 (2008).
33. J. F. Fleming, R. Feuda, N. W. Roberts, D. Pisani, A Novel Approach to Investigate the Effect of Tree Reconstruction Artifacts in Single-Gene Analysis Clarifies Opsin Evolution in Nonbilaterian Metazoans. *Genome Biology and Evolution* **12**, 3906–3916 (2020).

34. W. Han, *et al.*, Identification of eight genes encoding chemokine-like factor superfamily members 1–8 (CKLFSF1–8) by in silico cloning and experimental validation. *Genomics* **81**, 609–617 (2003).
35. H.-J. Duan, X.-Y. Li, C. Liu, X.-L. Deng, Chemokine-like factor-like MARVEL transmembrane domain-containing family in autoimmune diseases. *Chinese Medical Journal* **133** (2020).
36. S. F. Altschul, W. Gish, W. Miller, E. W. Myers, D. J. Lipman, Basic local alignment search tool. *Journal of Molecular Biology* **215**, 403–410 (1990).
37. S. F. Altschul, *et al.*, Gapped BLAST and PSI-BLAST: a new generation of protein database search programs. *Nucleic Acids Research* **25**, 3389–3402 (1997).
38. C. Camacho, *et al.*, BLAST+: architecture and applications. *BMC Bioinformatics* **10**, 421 (2009).
39. T. Frickey, A. Lupas, CLANS: a Java application for visualizing protein families based on pairwise similarity. *Bioinformatics* **20**, 3702–3704 (2004).
40. F. Gabler, *et al.*, Protein Sequence Analysis Using the MPI Bioinformatics Toolkit. *Current Protocols in Bioinformatics* **72**, e108 (2020).
41. J. L. Maravillas-Montero, *et al.*, Cutting Edge: GPR35/CXCR8 Is the Receptor of the Mucosal Chemokine CXCL17. *The Journal of Immunology* **194**, 29–33 (2015).
42. S.-J. Park, S.-J. Lee, S.-Y. Nam, D.-S. Im, GPR35 mediates lodoxamide-induced migration inhibitory response but not CXCL17-induced migration stimulatory response in THP-1 cells; is GPR35 a receptor for CXCL17? *British Journal of Pharmacology* **175**, 154–161 (2018).
43. N. A. S. B. M. Amir, *et al.*, Evidence for the Existence of a CXCL17 Receptor Distinct from GPR35. *The Journal of Immunology* **201**, 714–724 (2018).
44. B. Q. Minh, M. A. T. Nguyen, A. von Haeseler, Ultrafast Approximation for Phylogenetic Bootstrap. *Molecular Biology and Evolution* **30**, 1188–1195 (2013).
45. D. T. Hoang, O. Chernomor, A. von Haeseler, B. Q. Minh, L. S. Vinh, UFBoot2: Improving the Ultrafast Bootstrap Approximation. *Molecular Biology and Evolution* **35**, 518–522 (2018).
46. F. Lemoine, *et al.*, Renewing Felsenstein's phylogenetic bootstrap in the era of big data. *Nature* **556**, 452–456 (2018).
47. B. Morel, A. M. Kozlov, A. Stamatakis, G. J. Szöllősi, GeneRax: A Tool for Species-Tree-Aware Maximum Likelihood-Based Gene Family Tree Inference under Gene Duplication, Transfer, and Loss. *Molecular Biology and Evolution* **37**, 2763–2774 (2020).
48. T. A. Williams, *et al.*, The power and limitations of species tree-aware phylogenetics. 2023.03.17.533068 (2023).
49. H. Nomiyama, N. Osada, O. Yoshie, Systematic classification of vertebrate chemokines based on conserved synteny and evolutionary history. *Genes to Cells* **18**, 1–16 (2013).
50. A. Zlotnik, O. Yoshie, H. Nomiyama, The chemokine and chemokine receptor superfamilies and their molecular evolution. *Genome Biol* **7**, 243–243 (2006).
51. P. M. Murphy, "15 - Chemokines and Chemokine Receptors" in *Clinical Immunology (Sixth Edition)*, R. R. Rich, *et al.*, Eds. (Elsevier, 2023), pp. 215–227.

52. Z. Sun, *et al.*, The evolution and functional characterization of CXC chemokines and receptors in lamprey. *Developmental & Comparative Immunology* **116**, 103905 (2021).
53. A. Le Mercier, *et al.*, GPR182 is an endothelium-specific atypical chemokine receptor that maintains hematopoietic stem cell homeostasis. *Proceedings of the National Academy of Sciences* **118**, e2021596118 (2021).
54. P. Liò, M. Vannucci, Investigating the evolution and structure of chemokine receptors. *Gene* **317**, 29–37 (2003).
55. R. Fredriksson, M. C. Lagerström, L.-G. Lundin, H. B. Schiöth, The G-Protein-Coupled Receptors in the Human Genome Form Five Main Families. Phylogenetic Analysis, Paralogon Groups, and Fingerprints. *Mol Pharmacol* **63**, 1256–1272 (2003).
56. S. Xiao, W. Xie, L. Zhou, Mucosal chemokine CXCL17: What is known and not known. *Scandinavian Journal of Immunology* **93**, e12965 (2021).
57. S. P. Giblin, J. E. Pease, What defines a chemokine? – The curious case of CXCL17. *Cytokine* **168**, 156224 (2023).
58. J. Duan, *et al.*, Insights into divalent cation regulation and G13-coupling of orphan receptor GPR35. *Cell Discov* **8**, 1–12 (2022).
59. M. T. Pisabarro, *et al.*, Cutting Edge: Novel Human Dendritic Cell- and Monocyte-Attracting Chemokine-Like Protein Identified by Fold Recognition Methods. *The Journal of Immunology* **176**, 2069–2073 (2006).
60. E. J. Weinstein, *et al.*, VCC-1, a novel chemokine, promotes tumor growth. *Biochemical and Biophysical Research Communications* **350**, 74–81 (2006).
61. A. M. Najakshin, L. V. Mechetina, B. Y. Alabyev, A. V. Taranin, Identification of an IL-8 homolog in lamprey (Lampetra fluviatilis): early evolutionary divergence of chemokines. *European Journal of Immunology* **29**, 375–382 (1999).
62. B. Bajoghli, *et al.*, Evolution of Genetic Networks Underlying the Emergence of Thymopoiesis in Vertebrates. *Cell* **138**, 186–197 (2009).
63. L. Pan, J. Lv, Z. Zhang, Y. Zhang, Adaptation and Constraint in the Atypical Chemokine Receptor Family in Mammals. *BioMed Research International* **2018**, 9065181 (2018).
64. S. J. Allen, S. E. Crown, T. M. Handel, Chemokine:Receptor Structure, Interactions, and Antagonism. *Annual Review of Immunology* **25**, 787–820 (2007).
65. R. Horuk, *et al.*, A Receptor for the Malarial Parasite Plasmodium vivax: the Erythrocyte Chemokine Receptor. *Science* **261**, 1182–1184 (1993).
66. R. Horuk, The Duffy Antigen Receptor for Chemokines DARC/ACKR1. *Frontiers in Immunology* **6** (2015).
67. M. Kasahara, The 2R hypothesis: an update. *Current Opinion in Immunology* **19**, 547–552 (2007).
68. O. Simakov, *et al.*, Deeply conserved synteny resolves early events in vertebrate evolution. *Nat Ecol Evol* **4**, 820–830 (2020).
69. W. Tang, Y. Li, A. Li, M. E. Bronner, Clonal analysis and dynamic imaging identify multipotency of individual Gallus gallus caudal hindbrain neural crest cells toward cardiac and enteric fates. *Nat Commun* **12**, 1894 (2021).
70. J. R. York, D. W. McCauley, The origin and evolution of vertebrate neural crest cells. *Open Biology* **10**, 190285 (2020).

71. R. M. Waterhouse, *et al.*, BUSCO Applications from Quality Assessments to Gene Prediction and Phylogenomics. *Mol Biol Evol* **35**, 543–548 (2018).
72. M. Manni, M. R. Berkeley, M. Seppey, F. A. Simão, E. M. Zdobnov, BUSCO Update: Novel and Streamlined Workflows along with Broader and Deeper Phylogenetic Coverage for Scoring of Eukaryotic, Prokaryotic, and Viral Genomes. *Molecular Biology and Evolution* **38**, 4647–4654 (2021).
73. E. Boutet, *et al.*, "UniProtKB/Swiss-Prot, the Manually Annotated Section of the UniProt KnowledgeBase: How to Use the Entry View" in *Plant Bioinformatics: Methods and Protocols*, Methods in Molecular Biology., D. Edwards, Ed. (Springer, 2016), pp. 23–54.
74. S. Poux, *et al.*, On expert curation and scalability: UniProtKB/Swiss-Prot as a case study. *Bioinformatics* **33**, 3454–3460 (2017).
75. J. J. Smith, *et al.*, Sequencing of the sea lamprey (Petromyzon marinus) genome provides insights into vertebrate evolution. *Nat Genet* **45**, 415–421 (2013).
76. D. Yu, *et al.*, Hagfish genome illuminates vertebrate whole genome duplications and their evolutionary consequences. 2023.04.08.536076 (2023).
77. E. M. Zdobnov, R. Apweiler, InterProScan – an integration platform for the signature-recognition methods in InterPro. *Bioinformatics* **17**, 847–848 (2001).
78. P. Jones, *et al.*, InterProScan 5: genome-scale protein function classification. *Bioinformatics* **30**, 1236–1240 (2014).
79. F. Bachelerie, *et al.*, Chemokine receptors (version 2020.5) in the IUPHAR/BPS Guide to Pharmacology Database. *IUPHAR/BPS Guide to Pharmacology CITE* **2020** (2020).
80. The UniProt Consortium, UniProt: the Universal Protein Knowledgebase in 2023. *Nucleic Acids Research* **51**, D523–D531 (2023).
81. L. Käll, A. Krogh, E. L. L. Sonnhammer, Advantages of combined transmembrane topology and signal peptide prediction—the Phobius web server. *Nucleic Acids Research* **35**, W429–W432 (2007).
82. W. Li, L. Jaroszewski, A. Godzik, Clustering of highly homologous sequences to reduce the size of large protein databases. *Bioinformatics* **17**, 282–283 (2001).
83. L. Fu, B. Niu, Z. Zhu, S. Wu, W. Li, CD-HIT: accelerated for clustering the next-generation sequencing data. *Bioinformatics* **28**, 3150–3152 (2012).
84. G. Pándy-Szekeres, *et al.*, GPCRdb in 2023: state-specific structure models using AlphaFold2 and new ligand resources. *Nucleic Acids Research* **51**, D395–D402 (2023).
85. K. Katoh, K. Misawa, K. Kuma, T. Miyata, MAFFT: a novel method for rapid multiple sequence alignment based on fast Fourier transform. *Nucleic Acids Research* **30**, 3059–3066 (2002).
86. K. Katoh, D. M. Standley, MAFFT Multiple Sequence Alignment Software Version 7: Improvements in Performance and Usability. *Molecular Biology and Evolution* **30**, 772–780 (2013).
87. S. Capella-Gutiérrez, J. M. Silla-Martínez, T. Gabaldón, trimAl: a tool for automated alignment trimming in large-scale phylogenetic analyses. *Bioinformatics* **25**, 1972–1973 (2009).
88. B. Q. Minh, *et al.*, IQ-TREE 2: New Models and Efficient Methods for Phylogenetic Inference in the Genomic Era. *Molecular Biology and Evolution* **37**, 1530–1534 (2020).

89. S. Kalyaanamoorthy, B. Q. Minh, T. K. F. Wong, A. von Haeseler, L. S. Jermiin, ModelFinder: fast model selection for accurate phylogenetic estimates. *Nat Methods* **14**, 587–589 (2017).
90. J. Huerta-Cepas, F. Serra, P. Bork, ETE 3: Reconstruction, Analysis, and Visualization of Phylogenomic Data. *Molecular Biology and Evolution* **33**, 1635–1638 (2016).
91. W. Han, *et al.*, Molecular cloning and characterization of chemokine-like factor 1 (CKLF1), a novel human cytokine with unique structure and potential chemotactic activity. *Biochem J* **357**, 127–135 (2001).
92. L. Wang, *et al.*, Molecular cloning and characterization of chemokine-like factor super family member 1 (CKLFSF1), a novel human gene with at least 23 alternative splicing isoforms in testis tissue. *The International Journal of Biochemistry & Cell Biology* **36**, 1492–1501 (2004).
93. C. Jin, P. Ding, Y. Wang, D. Ma, Regulation of EGF receptor signaling by the MARVEL domain-containing protein CKLFSF8. *FEBS Letters* **579**, 6375–6382 (2005).
94. Z.-Z. Wang, *et al.*, Chemokine-like factor 1, a novel cytokine, induces nerve cell migration through the non-extracellular Ca2+-dependent tyrosine kinases pathway. *Brain Research* **1308**, 24–34 (2010).
95. T. Li, *et al.*, Expression of chemokine-like factor 1 is upregulated during T lymphocyte activation. *Life Sciences* **79**, 519–524 (2006).
96. Y. Zhang, *et al.*, C-terminal peptides of chemokine-like factor 1 signal through chemokine receptor CCR4 to cross-desensitize the CXCR4. *Biochemical and Biophysical Research Communications* **409**, 356–361 (2011).
97. H. Li, *et al.*, A novel 3p22.3 gene CMTM7 represses oncogenic EGFR signaling and inhibits cancer cell growth. *Oncogene* (2014) https:/doi.org/10.1038/onc.2013.282.
98. S. Zhu, *et al.*, Protein Cytl1: its role in chondrogenesis, cartilage homeostasis, and disease. *Cell. Mol. Life Sci.* **76**, 3515–3523 (2019).
99. H. Xue, *et al.*, CYTL1 Promotes the Activation of Neutrophils in a Sepsis Model. *Inflammation* **43**, 274–285 (2020).
100. X. Wang, *et al.*, Tafa-2 plays an essential role in neuronal survival and neurobiological function in mice. *Acta Biochimica et Biophysica Sinica* **50**, 984–995 (2018).
101. Y. Wang, *et al.*, Novel Adipokine, FAM19A5, Inhibits Neointima Formation After Injury Through Sphingosine-1-Phosphate Receptor 2. *Circulation* **138**, 48–63 (2018).
102. J. Okada, *et al.*, Analysis of FAM19A2/TAFA-2 function. *Physiology & Behavior* **208**, 112581 (2019).
103. B. L. Lokeshwar, G. Kallifatidis, J. J. Hoy, “Chapter One - Atypical chemokine receptors in tumor cell growth and metastasis” in *Advances in Cancer Research*, GPCR Signaling in Cancer., A. K. Shukla, Ed. (Academic Press, 2020), pp. 1–27.
104. H.-Q. He, R. D. Ye, The Formyl Peptide Receptors: Diversity of Ligands and Mechanism for Recognition. *Molecules* **22**, 455 (2017).
105. M. Dohrmann, G. Wörheide, Dating early animal evolution using phylogenomic data. *Sci Rep* **7**, 3599 (2017).
106. F. Delsuc, *et al.*, A phylogenomic framework and timescale for comparative studies of tunicates. *BMC Biol* **16**, 39 (2018).

107. F. M. Gradstein, J. G. Ogg, “Chapter 2 - The Chronostratigraphic Scale” in *The Geologic Time Scale*, F. M. Gradstein, J. G. Ogg, M. D. Schmitz, G. M. Ogg, Eds. (Elsevier, 2012), pp. 31–42.

	Names	Abbreviations	*H. sapiens* Orthologs	Functions	References
Ligand Groups	**Canonical Chemokines**	CCL, CXCL, XCL, CX3CL	CCL1-3, 3L1, 3L3, 4, 4L1-L2, 5, 7, 8, 11, 13, 14-28; CXCL1-4, 4L1, 5-14, 16,17; XCL1,2; CX3CL1	- Chemokine receptor binding and signalling - Chemoattraction of leukocytes - Homeostasis of leukocytes	(2, 4, 7)
	CKLF-Like MARVEL Transmembrane Domain-Containing Proteins (Chemokine-Like Factor Super Family)	CKLF, CMTM	CKLF1; CMTM1-8 (CKLF, CKLFSF1-8)	- CKLF1 (CKLF) binds to chemokine receptor CCR4 - CKLF1 (CKLF): chemotactic activity for lymphocytes, macrophages, and neutrophils - Other CMTMs: variably expressed in immune system; putative roles in immunity, programmed cell death, regulation of anti-tumour immunity etc.	(1, 10–12, 34, 35, 91–97)
	Cytokine-Like Protein 1 (Protein C17 or C4orf4)	CYTL	CYTL1	- Chemokine receptor binding (CCR2) and signalling - Chemoattraction monocytes/macrophages - Chemotactic activity in neutrophils	(1, 18, 98, 99)
	TAFA Chemokines (Family with sequence similarity 19 (chemokine (C-C motif)-like) member A)	TAFA	TAFA1-5 (FAM19A1-5)	- Formyl-peptide receptor binding and signalling (TAFA4 and 5) - Putative binding to other GPCRs: GPR1 (TAFA1); S1PR2 (TAFA5) - Expressed in central and peripheral nervous system - Implicated in vast diversity of physiological processes	(1, 13–17, 100–102)
Receptor Groups	**Canonical Chemokine Receptors**	CCR, CXCR, XCR, CX3CR	CCR1-10; CXCR1-6; XCR1; CX3CR1	- Chemokine binding and signalling - Chemotaxis of leukocytes - Homeostasis of leukocytes	(2, 4, 7)
	Atypical Chemokine Receptors	ACKR	ACKR1-4 (DARC; D6; CXCR7; CCRL1)	- Chemokine binding, but no signalling - Resolution of inflammatory response	(21, 27, 28)
	Chemokine Receptor-Like (Chemokine (C-C motif) receptor-like 2)	CCRL	CCRL2 (ACKR5)	- Binds CCL5 and CCL19, but no signalling - Binds chemerin and presents it to CMKLR1	(20, 103)
	Chemokine-Like Receptor 1	CML	CML1 (CMKLR1; ChemR23)	- Binds chemerin inducing migration of macrophages and dendritic cells - Binds also other anti-inflammatory molecules (e.g., Resolvin E1 (RvE1))	(20)
	Formyl-peptide Receptors	FPR	FPR 1-3	- TAFA chemokine binding - Chemoattraction, modulation of inflammation	(15, 16, 104)
	Putative Chemokine Receptors	ACKR6, CXCR8	PTITMP3, CXCR8 (GPR35)	- ACKR6/PTITMP3: Binds CCL18 (NB: It is not a GPCR) - CXCR8/GPR35: binds CXCL17	(41, 103)

Table 1: Summary table of all the canonical and non-canonical chemokine components analyzed in this study.

Figure Legends

Figure 1: Cluster Analysis and Phylogeny of Ligand groups. A) Similarity-based clustering, using CLANS, of canonical chemokines and related molecules with sequence similarity. Canonical chemokines are an independent group from other related molecules (TAFA, CYTL and CXCL17). Canonical chemokines are composed of two large groups (CC-type and CXC-type) within which some divergent subgroups are highlighted. The clustering and connections shown are at the p-value threshold of 1E-6. Other p-values tested are shown in Supplementary Figure S1. Candidate invertebrate sequences are shown as crosses and further information regarding them can be found in Supplementary Results. **B)** Similarity-based clustering, using CLANS, of the CKLF super family (CKLFSF). Two major clusters are formed: the smaller "CKLF Group I" and the heterogenous "CKLF group II" that also includes some invertebrate sequences (shown as crosses). Subclades, including the known members of the CKLF super family, are highlighted. The clustering and connections shown are at the p-value threshold of 1E-15, as this is the threshold at which the two major clusters connect. Other p-values tested are shown in Supplementary Figure S2. **C)** Maximum-Likelihood un-rooted phylogenetic tree of canonical chemokines. CC-type and CXC-type are split into two separate clades. Supports for key nodes are indicated in boxes with Transferable Bootstrap Expectation (TBE) represented by triangles and the Ultrafast Bootstraps (UFB) as circles. A traffic light colour code is used to indicate the level of support: high (green); intermediate (yellow) and low (red). **D)** Maximum-Likelihood un-rooted phylogenetic tree of the CKLF super family (CKLFSF). The CKLF group I is monophyletic, while the CKLF group II is not. Supports for key nodes are indicated in boxes with Transferable Bootstrap Expectation (TBE) represented by triangles and the Ultrafast Bootstraps

763 (UFB) as circles. A traffic light colour code is used to indicate the level of support: high (green);
764 intermediate (yellow) and low (red).
765
766 **Figure 2: Distribution and duplication patterns of ligand groups. A)** Presence of all ligand groups are
767 mapped onto a species tree. Gene trees and duplication events are based on the gene tree to
768 species tree reconciliation analyses. The nomenclature for canonical chemokines is primarily based
769 on known chemokines of human (or mouse). Where human and mouse chemokines do not
770 correspond, the default name refers to the human gene and the mouse (*Mus musculus*) one is
771 indicated with "Mm". Chemokines that have been classically described as having either homeostatic
772 or inflammatory function are indicated with a circle or a star respectively. The classification used
773 here was based on Zlotnik and Yoshie 2012 (7) with the inflammatory type also including
774 chemokines they described as plasma/platelet types. Overall, canonical chemokines originated in
775 vertebrates and expanded a first time in jawed vertebrates and a second time in mammals.
776 Homeostatic chemokines (e.g., CXCL12) are generally more ancient than inflammatory ones. CXCL17
777 and CYTL are mammal and jawed vertebrate specific respectively. TAFA originated in the common
778 ancestor of vertebrates and urochordates, while the CKLF super family is present in invertebrates
779 although key duplications occurred at the base of vertebrates. **B)** Number of complements for each
780 ligand group at key species nodes are mapped onto the species tree. The number of complements in
781 each group reflects the pattern of duplications. The major increase occurred at the level of jawed
782 vertebrates with canonical chemokines undergoing a second significant increase within placentals.
783 Silhouette images are by Andreas Hejnol (*Xenopus laevis*); Andy Wilson (*Anas platyrhynchos*,
784 *Taeniopygia guttata*); Carlos Cano-Barbacil (*Salmo trutta*); Christoph Schomburg (*Anolis carolinensis*,
785 *Ciona intestinalis*, *Eptatretus burgeri*, *Petromyzon marinus*); Christopher Kenaley (*Mola mola*);
786 Chuanixn Yu (*Latimeria chalumnae*); Daniel Jaron (*Mus musculus*); Daniel Stadtmauer (*Monodelphis*
787 *domestica*); Fernando Carezzano (Asteroidea); Ingo Braasch (*Callorhinchus milii*); Jake Warner (*Danio*
788 *rerio*); Kamil S. Jaron (*Poecilia formosa*); Mali'o Kodis, photograph by Hans Hillewaert

(*Branchiostoma lanceolatum*, https://www.phylopic.org/images/719d7b41-cedc-4c97-9ffe-dd8809f85553/branchiostoma-lanceolatum); Margot Michaud (*Canis lupus*, *Physeter macrocephalus*); NASA (*Homo sapiens sapiens*); Nathan Hermann (*Scophthalmus aquosus*); Ryan Cupo (*Rattus norvegicus*); seung9park (*Takifugu rubripes rubripes*); Soledad Miranda-Rottmann (*Pelodiscus sinensis*, https://www.phylopic.org/images/929fd134-bbd7-4744-987f-1975107029f5/pelodiscus-sinensis); Steven Traver (*Gallus gallus domesticus*, *Ornithorhynchus anatinus*); Stuart Humphries (*Thunnus thynnus*); T. Michael Keesey (after Colin M. L. Burnett) (*Gorilla gorilla gorilla*); Thomas Hegna (based on picture by Nicolas Gompel) (*Drosophila (Drosophila) mojavensis*); and Yan Wong (*Balanoglossus*).

Figure 3: Phylogeny of Receptor groups.

An unrooted maximum likelihood phylogeny of chemokine receptors. The tree shown is the transfer bootstrap expectation (TBE) tree including just the chordate specific clade from the ultrafast bootstrap tree (UFB). Node supports from both TBE (triangle) and UFB (circle) shown for equivalent key nodes in boxes with arrows to indicate node. A traffic light colour code is used to indicate the level of support: high (green); intermediate (yellow) and low (red). Key clades highlighted: yellow = chemokine like plus group (CMLplus); blue = intermediate group; green = atypical 3 and GPR182 (ACKR3/GPR182); purple = canonical chemokines (Canonical CKR); and pink = relaxin receptors (RL3R). Branches scaled by amino acid substitutions per site.

Figure 4: Distribution and duplication patterns of receptor groups.

A) Presence of all receptor groups are mapped onto a species tree. Gene trees and duplication events are based on the gene tree to species tree reconciliation analyses. The nomenclature for genes is primarily based on human chemokines. The canonical chemokines had 5 paralogs present in the vertebrate common ancestor. These undergo a heterogeneous pattern of duplication throughout vertebrates with different paralogs duplicating different number of times and in

different groups of species. Chemokines that have been classically described as having either homeostatic or inflammatory function are indicated with a circle or a star respectively. The classification used here was based on Zlotnik and Yoshie 2012 (7). **B)** Number of complements for each receptor group at key species nodes are mapped onto the species tree. The number of complements in each group reflects the pattern of duplications. The chemokine groups diverged in the vertebrate stem group. The major expansion occurred at the level of jawed vertebrates with canonical chemokine receptors, the chemokine-like receptor plus group and intermediate groups increasing in copy number. Canonical chemokine underwent another small subsequent increase within placentals. Silhouette images are by Andreas Hejnol (*Xenopus laevis*); Andy Wilson (*Anas platyrhynchos*, *Taeniopygia guttata*); Carlos Cano-Barbacil (*Salmo trutta*); Christoph Schomburg (*Anolis carolinensis*, *Ciona intestinalis*, *Eptatretus burgeri*, *Petromyzon marinus*); Christopher Kenaley (*Mola mola*); Chuanixn Yu (*Latimeria chalumnae*); Daniel Jaron (*Mus musculus*); Daniel Stadtmauer (*Monodelphis domestica*); Fernando Carezzano (Asteroidea); Ingo Braasch (*Callorhinchus milii*); Jake Warner (*Danio rerio*); Kamil S. Jaron (*Poecilia formosa*); Mali'o Kodis, photograph by Hans Hillewaert (*Branchiostoma lanceolatum*, https://www.phylopic.org/images/719d7b41-cedc-4c97-9ffe-dd8809f85553/branchiostoma-lanceolatum); Margot Michaud (*Canis lupus*, *Physeter macrocephalus*); NASA (*Homo sapiens sapiens*); Nathan Hermann (*Scophthalmus aquosus*); Ryan Cupo (*Rattus norvegicus*); seung9park (*Takifugu rubripes rubripes*); Soledad Miranda-Rottmann (*Pelodiscus sinensis*, https://www.phylopic.org/images/929fd134-bbd7-4744-987f-1975107029f5/pelodiscus-sinensis); Steven Traver (*Gallus gallus domesticus*, *Ornithorhynchus anatinus*); Stuart Humphries (*Thunnus thynnus*); T. Michael Keesey (after Colin M. L. Burnett) (*Gorilla gorilla gorilla*); Thomas Hegna (based on picture by Nicolas Gompel) (*Drosophila (Drosophila) mojavensis*); and Yan Wong (*Balanoglossus*).

Figure 5: Summary of the evolution of ligands and receptors.

A summary diagram of the evolution of the different chemokine system components. A simplified phylogenetic tree of species is shown, calibrated to time according to Dohrmann and Wörheide 2017 (105) for Deuterostomia and Bilateria nodes and Delsuc et al. 2018 (106) for all other nodes. Circles represent ligand groups, and 7 transmembrane domain structure icons represent GPCR groups. Icons are colour coded by group, and placed adjacent to the branch in the species tree where they first appear. X2 and X5 indicate the number of paralogs present for CXCL ligand group and the canonical CKR groups respectively, on the branch where they first appear. Question mark refers to the uncertainty regarding the origin of the CKLF group I in jawed vertebrates or deuterostome stem group (see Figure 2). Geological column is shown along the bottom, in accordance with the ICS International Chronostratigraphic Chart (107).

Supplementary Tables:

Table S1. List of the species used in this work and their respective BUSCO values and accession number.

Table S2. Substitution models used in the phylogenetic analyses.

Supplementary Figure captions:

Figure S1. CLANS clustering of chemokines and related molecules sequences. Initial identification and annotation of clusters was performed at the strict p-value of 1E-35 **(A)**. Subsequent loosening of the p-value clarified the relationships across clusters and defined bigger groups. At p-value 1E-15 **(B)** two major canonical chemokine groups are well-defined: the CCL group, which includes also XCL and X3CL; and the CXCL group. At this level of stringency, only few canonical chemokines remain isolated: CCL27/28; CXCL12; CXCL14; CXCL16; as well as CXCL17. TAFA and CYTL are also isolated. At p-value 1E-10 **(C)** the two major chemokine groups connect to each other. CCL27/28 is connected to the CCL group and CXCL12 and CXCL14 are connected to the CXCL group, while CXCL16 and CXCL17 are still isolated. At p-value 1E-6 **(D)** all chemokine groups are connected in one big cluster, except for CXCL17. TAFA and CYTL are also still isolated. Crosses indicate the few invertebrate sequences that were collected from the BLAST search, more information in Supplementary Results.

Figure S2. CLANS clustering of CKLF Super Family sequences. Initial identification and annotation of clusters was performed at the strict p-value of 1E-60 **(A)**. Subsequent loosening of the p-value clarified the relationships across clusters and defined bigger groups. At 1E-20 **(B)** two major clusters have formed. One, that we called CKLF group I, includes CKLF, CMTM1,2,3,5, and PLP2. The other, that we called CKLF group II, includes CMTM4/6,7,8, and other groups. At 1E-16 **(C)** more sequences have joined the two major groups that are still separate. At 1E-15 **(D)** the two major groups connect,

as well as few extra sequences, see Supplementary Results for extra details. Crosses indicate invertebrate sequences.

Figure S3. Alignment of candidate brachiopod CCL24 sequence with mammalian CCL24s. Our BLAST searches picked up a sequence from the brachiopod *Lingula unguis* that when re-blasted versus SwissProt returned a CCL24 as hit. Alignment of the brachiopod sequence with mammalian CCL24 sequences reveals a poor overall conservation, with the brachiopod sequence also being significantly longer than any of the other sequences. Further details about this sequence can be found in supplementary file S3 and in Supplementary Results.

Figure S4. Alignment of candidate cnidarian CCL3 sequence with mammalian CCL3s. Our BLAST searches picked up a sequence from the cnidarian *Clytia hemisphaerica* that when re-blasted versus SwissProt returned a CCL3 as hit. Alignment of the cnidarian sequence with mammalian CCL3 sequences reveals a poor overall conservation, with the cnidarian sequence being extremely longer than any of the other sequences. Further details about this sequence can be found in supplementary file S3 and in Supplementary Results.

Figure S5. Alignment of candidate echinoderm CXCL10 sequence with mammalian CXCL10s. Our BLAST searches picked up a sequence from the echinoderm *Acanthaster planci* that when re-blasted versus SwissProt returned a CXCL10 as hit. Alignment of the echinoderm sequence with mammalian CXCL10 sequences reveals a poor overall conservation, with the brachiopod sequence also being significantly longer than any of the other sequences. Further details about this sequence can be found in supplementary file S3 and in Supplementary Results.

Figure S6. Alignment of 4 candidate urochordate TAFA sequences with vertebrate TAFAs. Our BLAST searches picked up 4 sequences from the urochordate *Ciona intestinalis*, that connected with

the TAFA cluster in the CLANS analysis. One of these sequences when blasted versus SwissProt returned a TAFA as hit. This sequence was also annotated as TAFA by InterProScan. Alignment of the urochordate sequences with vertebrate TAFA sequences reveals that only the one annotated as TAFA aligns well. While the other 3 align poorly and are also significantly longer than any of the other sequences. Further details about these sequences can be found in supplementary file S3 and in Supplementary Results.

Figure S7. Alignment of best candidate urochordate TAFA sequence with vertebrate TAFAs. Of the 4 urochordate candidate TAFA sequences, only one was annotated as TAFA with both SwissProt and InterProScan annotation and appeared to align well with other TAFAs with a preliminary alignment with all urochordate sequences (Figure S6). Here we removed the other 3 urochordate sequences and aligned only the best candidate with the vertebrate TAFAs. The sequence conservation is even more apparent with this alignment. Importantly, 8 of the 10 typical cysteine residues of TAFA1-4 are conserved, and the two missing cysteines are the same ones missing in TAFA5. Further discussion can be found in Supplementary Results.

Figure S8. Unrooted phylogenetic tree of canonical chemokines with TBE supports. Phylogenetic tree under the model GTR20+F+R4. Nodal support is calculated from 100 non-parametric bootstrap repeats with transferable bootstrap expectation. CCL clade is in orange, CXCL clade in blue.

Figure S9. Unrooted phylogenetic tree of canonical chemokines with UFB supports. Phylogenetic tree under the model GTR20+F+R4. Nodal support is calculated from 1000 ultrafast bootstrap repeats. CCL clade is in orange, CXCL clade in blue.

Figure S10. Unrooted phylogenetic tree of TAFA with TBE supports. Phylogenetic tree under the model JTT+R5. Nodal support is calculated from 100 non-parametric bootstrap repeats with transferable bootstrap expectation.

Figure S11. Unrooted phylogenetic tree of TAFA with UFB supports. Phylogenetic tree under the model JTT+R5. Nodal support is calculated from 1000 ultrafast bootstrap repeats.

Figure S12. Unrooted phylogenetic tree of CYTL with TBE supports. Phylogenetic tree under the model JTT+I+G4. Nodal support is calculated from 100 non-parametric bootstrap repeats with transferable bootstrap expectation.

Figure S13. Unrooted phylogenetic tree of CYTL with UFB supports. Phylogenetic tree under the model JTT+I+G4. Nodal support is calculated from 1000 ultrafast bootstrap repeats.

Figure S14. Unrooted phylogenetic tree of CXCL17 with TBE supports. Phylogenetic tree under the model JTT. Nodal support is calculated from 100 non-parametric bootstrap repeats with transferable bootstrap expectation.

Figure S15. Unrooted phylogenetic tree of CXCL17 with UFB supports. Phylogenetic tree under the model JTT. Nodal support is calculated from 1000 ultrafast bootstrap repeats.

Figure S16. Unrooted phylogenetic tree of CKLFSF with TBE supports. Phylogenetic tree under the model GTR20+F+R7. Nodal support is calculated from 100 non-parametric bootstrap repeats with transferable bootstrap expectation. Red clade = CMTM4/6; blue clade = CKLF I group; green clade = CMTM7; turquois clade = MAL/MALL/MAL2.

Figure S17. Unrooted phylogenetic tree of CKLFSF with UFB supports. Phylogenetic tree under the model GTR20+F+R7. Nodal support is calculated from 1000 ultrafast bootstrap repeats. Red clade = CMTM4/6; blue clade = CKLF I group; green clade = CMTM7; turquois clade = MAL/MALL/MAL2.

Figure S18. Rooted species tree reconciled gene tree for canonical chemokines. The canonical chemokines gene tree was reconciled with the species tree using GeneRax. "S" or "D" at the node indicates a speciation or duplication event respectively. CCL clade is in orange, CXCL clade in blue.

Figure S19. Rooted species tree reconciled gene tree for TAFA. The TAFA gene tree was reconciled with the species tree using GeneRax. "S" or "D" at the node indicates a speciation or duplication event respectively.

Figure S20. Rooted species tree reconciled gene tree for CYTL. The CYTL gene tree was reconciled with the species tree using GeneRax. "S" or "D" at the node indicates a speciation or duplication event respectively.

Figure S21. Rooted species tree reconciled gene tree for CXCL17. The CXCL17 gene tree was reconciled with the species tree using GeneRax. "S" or "D" at the node indicates a speciation or duplication event respectively.

Figure S22. Rooted species tree reconciled gene tree for CKLFSF. The CKLFSF gene tree was reconciled with the species tree using GeneRax. "S" or "D" at the node indicates a speciation or duplication event respectively. Red clade = CMTM4/6; blue clade = CKLF I group; green clade = CMTM7; turquois clade = MAL/MALL/MAL2.

Figure S23. CLANS clustering of receptors and related molecules sequences. A CLANS clustering layout where shapes indicate sequences and lines are connections indicating similarity between sequences at or surpassing the p-value similarity threshold. Sequences are positioned in clusters based on similarity. Initial identification and annotation of clusters was performed using the inbuilt convex clustering at the p-value of 1E-100. **(A)** clustering was loosened till the canonical receptor annotated groups formed a cluster at 1E-65. **(B)** loosening of the p-value to 1E-60 identified relationships between clusters of interest and identified the intermediate group as connecting to both canonical and chemokine-like plus groups. All sequences connected to groups of interest are vertebrate sequences. **(C)** further loosening to p-value 1E-50 connects the vertebrate sequences of interest to a large cluster of sequences which contains vertebrate and invertebrate sequences which are annotated as opioid and somatostatin receptors and other GPCRs. Crosses indicate invertebrate sequences and Y-shape indicates the reference viral sequences included. Shapes are colour coded by group of interest: purple = canonical chemokine receptors; yellow = chemokine-like plus; green = atypical receptor 3/GPR182; blue = intermediate group; pink = relaxin receptors.

Figure S24. Unrooted phylogenetic tree of receptors with TBE supports. Phylogenetic tree of receptor sequences of interest and putative outgroups under the model GTR20+F+G4. Sequences used are a subset of sequences extracted from CLANs, specifically they are those in the chordate specific clade in the ultrafast bootstrap tree. Nodal support is calculated from 100 non-parametric bootstrap repeats with transferable bootstrap expectation. Branches colour coded by group of interest: purple = canonical chemokine receptors; yellow = chemokine-like plus; green = atypical receptor 3/GPR182; blue = intermediate group; pink = relaxin receptors.

Figure S25. Unrooted phylogenetic tree of receptors with UFB supports. Phylogenetic tree of all receptor sequences of interest and putative outgroups extracted from clans under the model GTR20+F+G4. Nodal support is calculated from 1000 ultrafast bootstrap repeats. Branches colour

coded by group of interest: purple = canonical chemokine receptors; yellow = chemokine-like plus; green = atypical receptor 3/GPR182; blue = intermediate group; pink = relaxin receptors.

Figure S26. Rooted species tree reconciled gene tree for receptors. The ultrafast bootstrap receptor tree was modified to extract the subtree of the chordate specific clade. This gene tree was reconciled with the species tree using GeneRax. “S” or “D” at the node indicates a speciation or duplication event respectively. Branches colour coded by group of interest: purple = canonical chemokine receptors; yellow = chemokine-like plus; green = atypical receptor 3/GPR182; blue = intermediate group; pink = relaxin receptors.

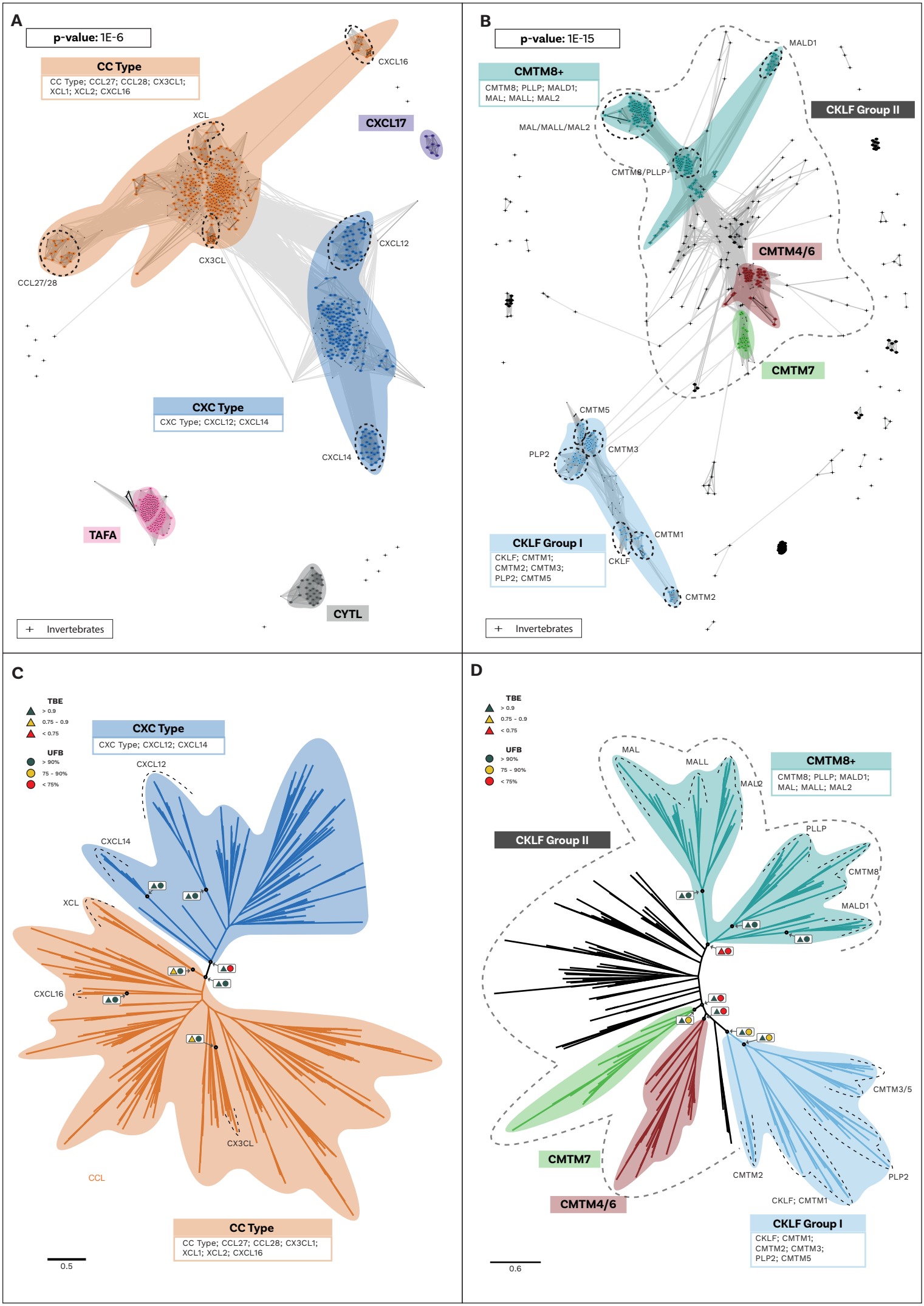
A
p-value: 1E-6
CC Type
CC Type; CCL27; CCL28; CX3CL1; XCL1; XCL2; CXCL16
CXCL16
XCL
CXCL17
CXCL12
CX3CL
CCL27/28
CXC Type
CXC Type; CXCL12; CXCL14
CXCL14
TAFA
CYTL
+ Invertebrates
B
p-value: 1E-15
CMTM8+
CMTM8; PLLP; MALD1; MAL; MALL; MAL2
MALD1
CKLF Group II
MAL/MALL/MAL2
CMTM8/PLLP
CMTM4/6
CMTM7
CMTM5
PLP2
CMTM3
CMTM1
CKLF
CKLF Group I
CKLF; CMTM1; CMTM2; CMTM3; PLP2; CMTM5
CMTM2
+ Invertebrates
C
TBE
> 0.9
0.75 - 0.9
< 0.75
UFB
> 90%
75 - 90%
< 75%
CXC Type
CXC Type; CXCL12; CXCL14
CXCL12
CXCL14
XCL
CXCL16
CX3CL
CCL
CC Type
CC Type; CCL27; CCL28; CX3CL1; XCL1; XCL2; CXCL16
0.5
D
TBE
> 0.9
0.75 - 0.9
< 0.75
UFB
> 90%
75 - 90%
< 75%
MAL
MALL
MAL2
CMTM8+
CMTM8; PLLP; MALD1; MAL; MALL; MAL2
CKLF Group II
PLLP
CMTM8
MALD1
CMTM3/5
CMTM7
CMTM2
PLP2
CMTM4/6
CKLF; CMTM1
CKLF Group I
CKLF; CMTM1; CMTM2; CMTM3; PLP2; CMTM5
0.6

Fig. 2

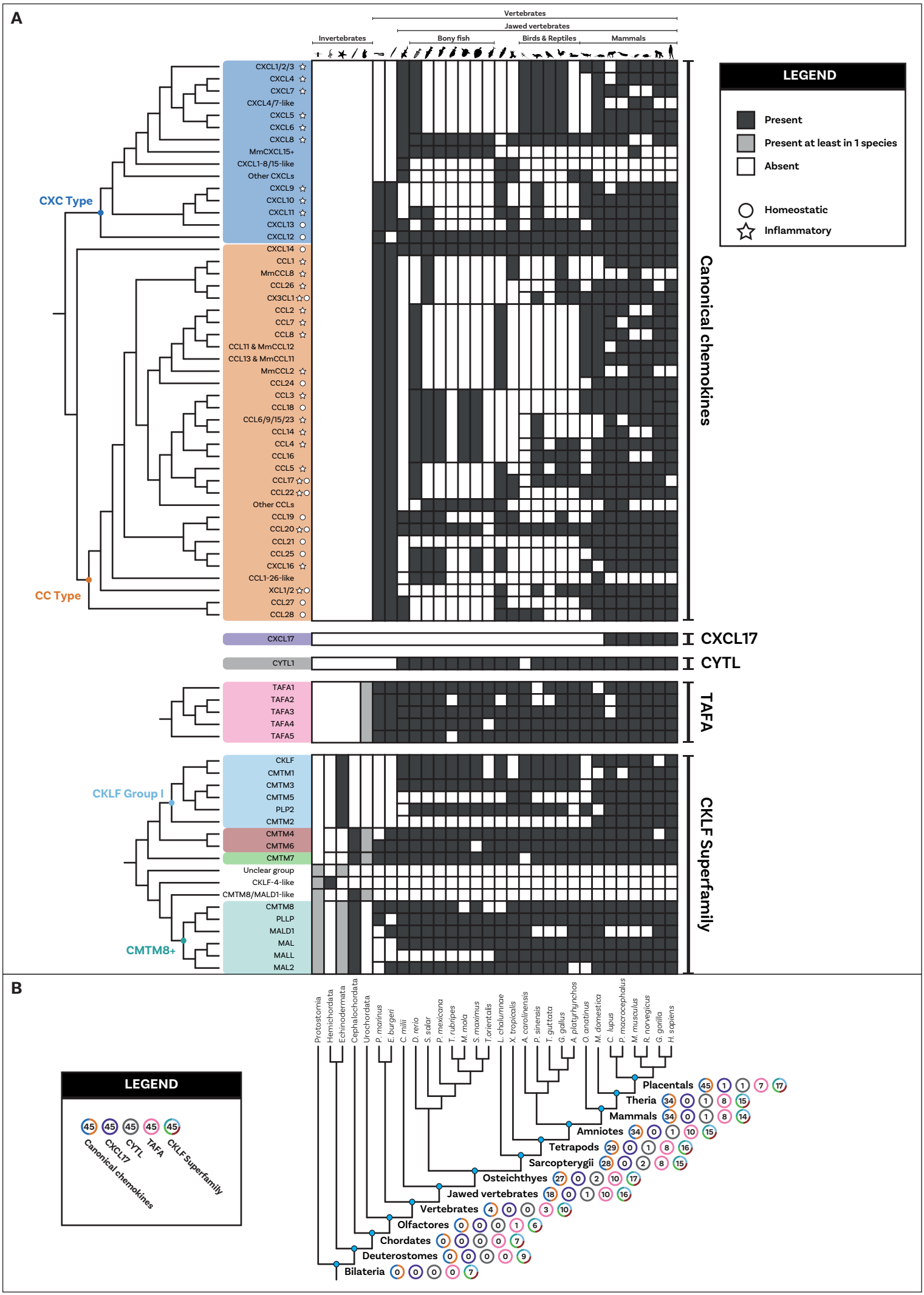
A
Vertebrates
Jawed vertebrates
Invertebrates
Bony fish
Birds & Reptiles
Mammals
CXC Type
CC Type
CXCL1/2/3
CXCL4
CXCL7
CXCL4/7-like
CXCL5
CXCL6
CXCL8
MmCXCL15+
CXCL1-8/15-like
Other CXCLs
CXCL9
CXCL10
CXCL11
CXCL13
CXCL12
CXCL14
CCL1
MmCCL8
CCL26
CX3CL1
CCL2
CCL7
CCL8
CCL11 & MmCCL12
CCL13 & MmCCL11
MmCCL2
CCL24
CCL3
CCL18
CCL6/9/15/23
CCL14
CCL4
CCL16
CCL5
CCL17
CCL22
Other CCLs
CCL19
CCL20
CCL21
CCL25
CXCL16
CCL1-26-like
XCL1/2
CCL27
CCL28
Canonical chemokines
CXCL17
CXCL17
CYTL1
CYTL
TAFA1
TAFA2
TAFA3
TAFA4
TAFA5
TAFA
CKLF Group I
CKLF
CMTM1
CMTM3
CMTM5
PLP2
CMTM2
CMTM4
CMTM6
CMTM7
Unclear group
CKLF-4-like
CMTM8/MALD1-like
CMTM8+
CMTM8
PLLP
MALD1
MAL
MALL
MAL2
CKLF Superfamily
LEGEND
Present
Present at least in 1 species
Absent
Homeostatic
Inflammatory
B
Protostomia
Hemichordata
Echinodermata
Cephalochordata
Urochordata
P. marinus
E. burgeri
C. milii
D. rerio
S. salar
P. mexicana
T. rubripes
M. mola
S. maximus
T. orientalis
L. chalumnae
X. tropicalis
A. carolinensis
P. sinensis
T. guttata
G. gallus
A. platyrhynchos
O. anatinus
M. domestica
C. lupus
P. macrocephalus
M. musculus
R. norvegicus
G. gorilla
H. sapiens
Placentals 45 1 1 7 17
Theria 34 0 1 8 15
Mammals 34 0 1 8 14
Amniotes 34 0 1 10 15
Tetrapods 29 0 1 8 16
Sarcopterygii 28 0 2 8 15
Osteichthyes 27 0 2 10 17
Jawed vertebrates 18 0 1 10 16
Vertebrates 4 0 0 3 10
Olfactores 0 0 0 1 6
Chordates 0 0 0 0 7
Deuterostomes 0 0 0 0 9
Bilateria 0 0 0 0 7
LEGEND
45 Canonical chemokines
45 CXCL17
45 CYTL
45 TAFA
45 CKLF Superfamily

Fig. 3

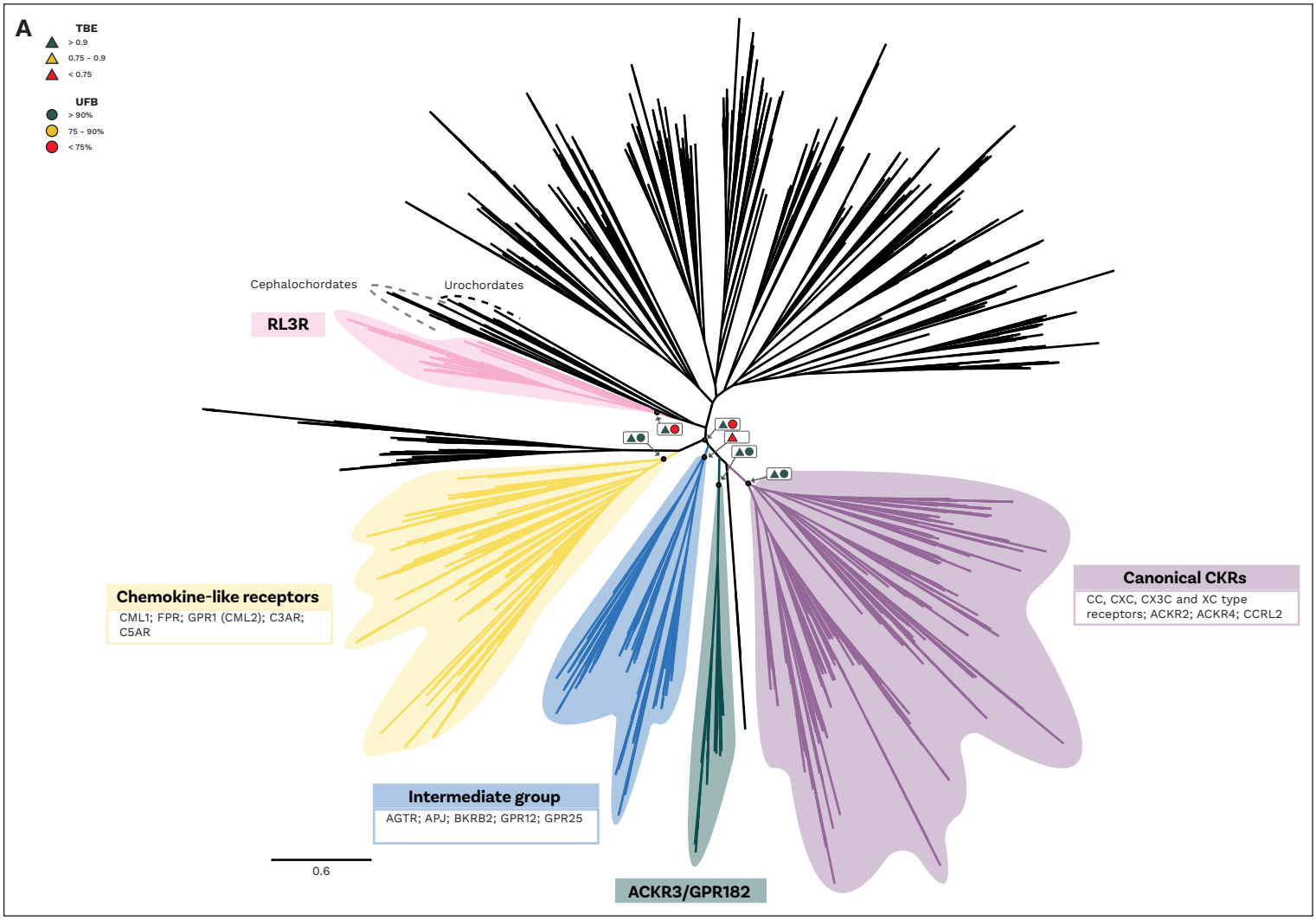
A
TBE
> 0.9
0.75 - 0.9
< 0.75
UFB
> 90%
75 - 90%
< 75%
Cephalochordates
Urochordates
RL3R
Chemokine-like receptors
CML1; FPR; GPR1 (CML2); C3AR; C5AR
Intermediate group
AGTR; APJ; BKRB2; GPR12; GPR25
ACKR3/GPR182
Canonical CKRs
CC, CXC, CX3C and XC type receptors; ACKR2; ACKR4; CCRL2
0.6

Fig. 4

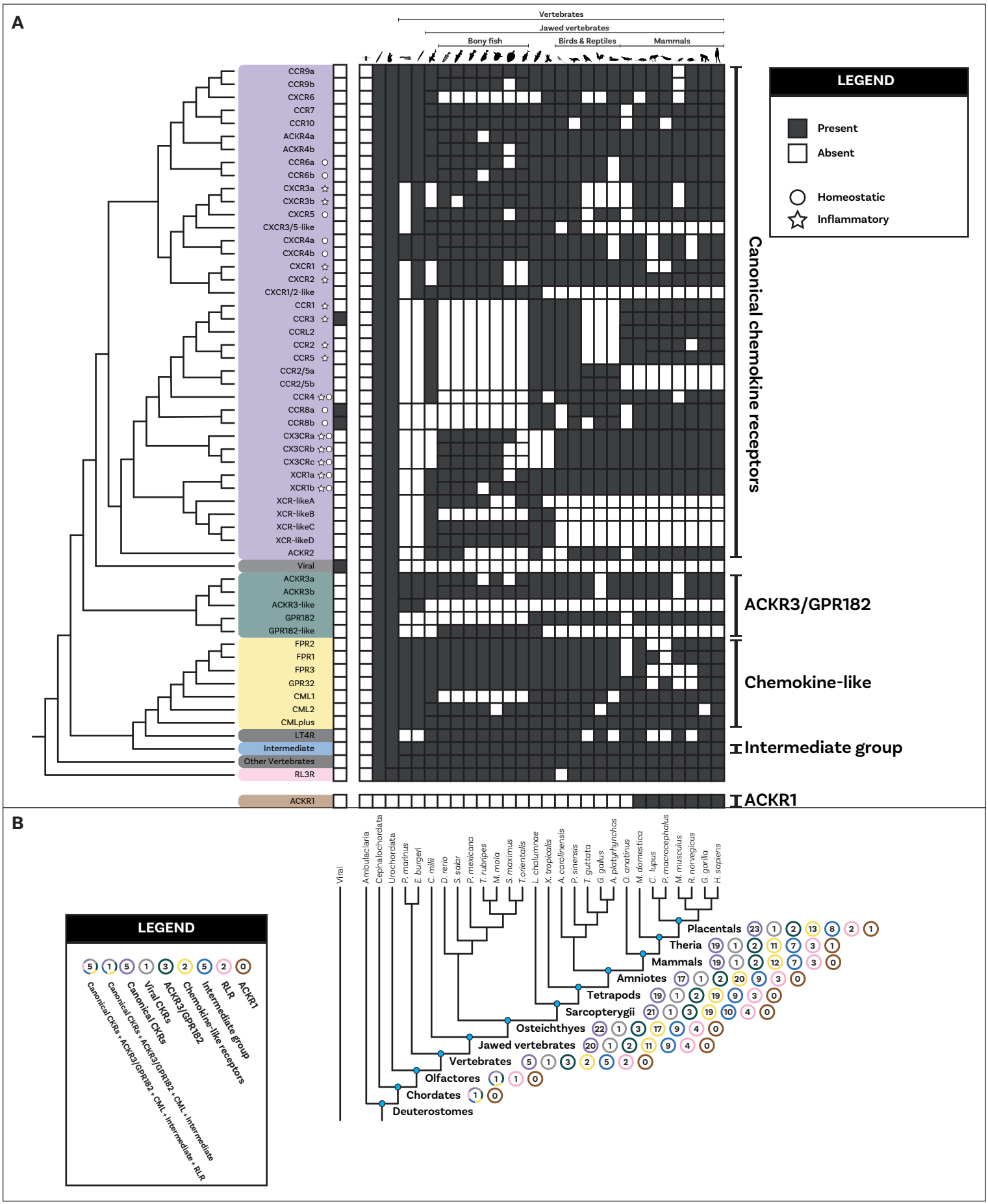
A
Vertebrates
Jawed vertebrates
Bony fish
Birds & Reptiles
Mammals
CCR9a
CCR9b
CXCR6
CCR7
CCR10
ACKR4a
ACKR4b
CCR6a
CCR6b
CXCR3a
CXCR3b
CXCR5
CXCR3/5-like
CXCR4a
CXCR4b
CXCR1
CXCR2
CXCR1/2-like
CCR1
CCR3
CCRL2
CCR2
CCR5
CCR2/5a
CCR2/5b
CCR4
CCR8a
CCR8b
CX3CRa
CX3CRb
CX3CRc
XCR1a
XCR1b
XCR-likeA
XCR-likeB
XCR-likeC
XCR-likeD
ACKR2
Viral
ACKR3a
ACKR3b
ACKR3-like
GPR182
GPR182-like
FPR2
FPR1
FPR3
GPR32
CML1
CML2
CMLplus
LT4R
Intermediate
Other Vertebrates
RL3R
ACKR1
LEGEND
Present
Absent
Homeostatic
Inflammatory
Canonical chemokine receptors
ACKR3/GPR182
Chemokine-like
Intermediate group
ACKR1
B
Viral
Ambulacraria
Cephalochordata
Urochordata
P. marinus
E. burgeri
C. milii
D. rerio
S. salar
P. mexicana
T. rubripes
M. mola
S. maximus
T. orientalis
L. chalumnae
X. tropicalis
A. carolinensis
P. sinensis
T. guttata
G. gallus
A. platyrhynchos
O. anatinus
M. domestica
C. lupus
P. macrocephalus
M. musculus
R. norvegicus
G. gorilla
H. sapens
Placentals 23 1 2 13 8 2 1
Theria 19 1 2 11 7 3 1
Mammals 19 1 2 12 7 3 0
Amniotes 17 1 2 20 9 3 0
Tetrapods 19 1 2 19 9 3 0
Sarcopterygii 21 1 3 19 10 4 0
Osteichthyes 22 1 3 17 9 4 0
Jawed vertebrates 20 1 2 11 9 4 0
Vertebrates 5 1 3 2 5 2 0
Olfactores 1 1 0
Chordates 1 0
Deuterostomes
LEGEND
5 1 5 1 3 2 5 2 0
Canonical CKRs + ACKR3/GPR182 + CML + Intermediate + RLR
Canonical CKRs + ACKR3/GPR182 + CML + Intermediate
Canonical CKRs
Viral CKRs
ACKR3/GPR182
Chemokine-like receptors
Intermediate group
RLR
ACKR1

Fig. 5

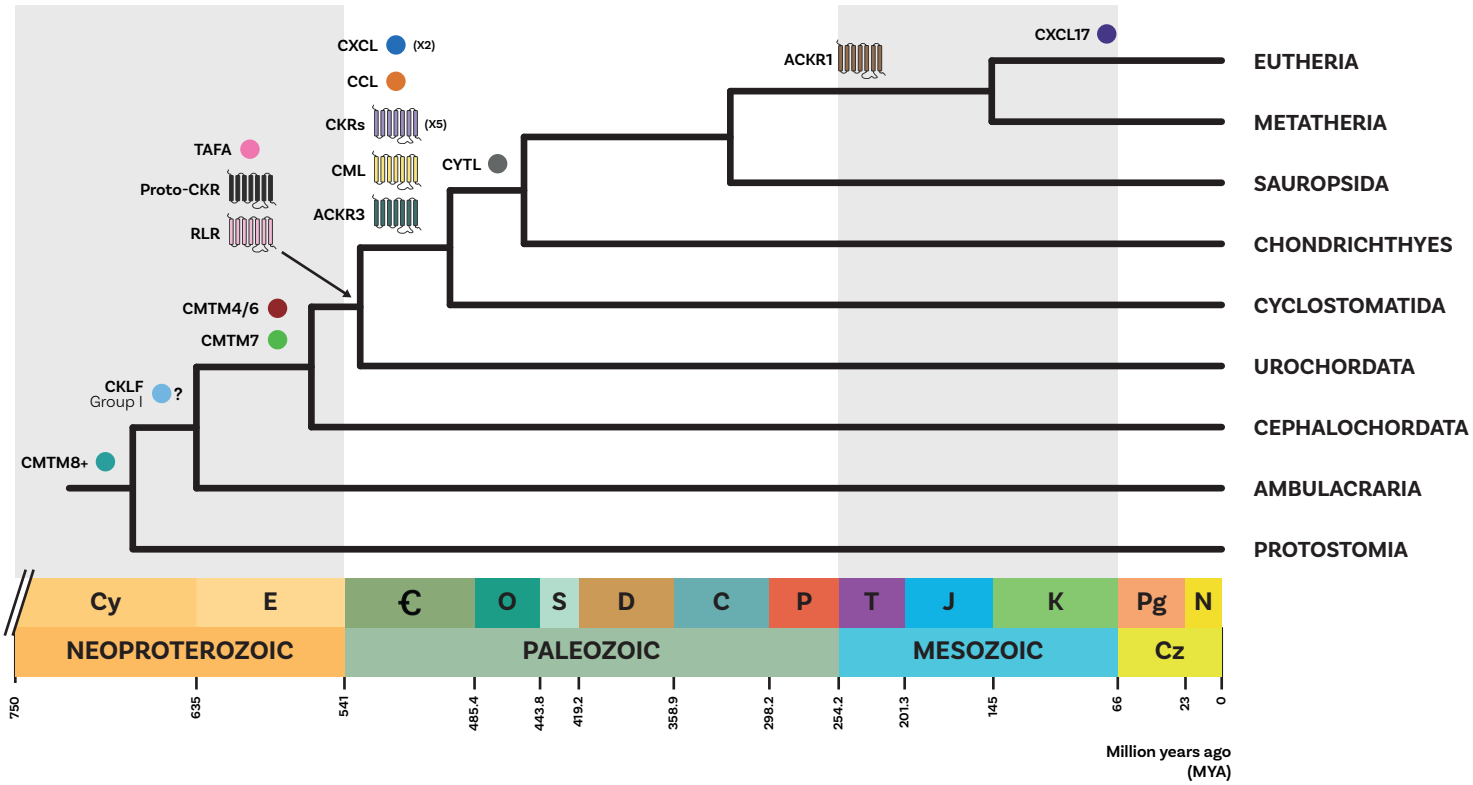
CXCL (X2)
CCL
CKRs (X5)
CML
ACKR3
TAFA
Proto-CKR
RLR
CYTL
ACKR1
CXCL17
CMTM4/6
CMTM7
CKLF
Group I
?
CMTM8+
EUTHERIA
METATHERIA
SAUROPSIDA
CHONDRICHTHYES
CYCLOSTOMATIDA
UROCHORDATA
CEPHALOCHORDATA
AMBULACRARIA
PROTOSTOMIA
Cy
E
Є
O
S
D
C
P
T
J
K
Pg
N
NEOPROTEROZOIC
PALEOZOIC
MESOZOIC
Cz
750
635
541
485.4
443.8
419.2
358.9
298.2
254.2
201.3
145
66
23
0
Million years ago
(MYA)